Extending the reach and capabilities of a superconducting quantum testbed

Ravi K. Naik

Lawrence Berkeley National Laboratory

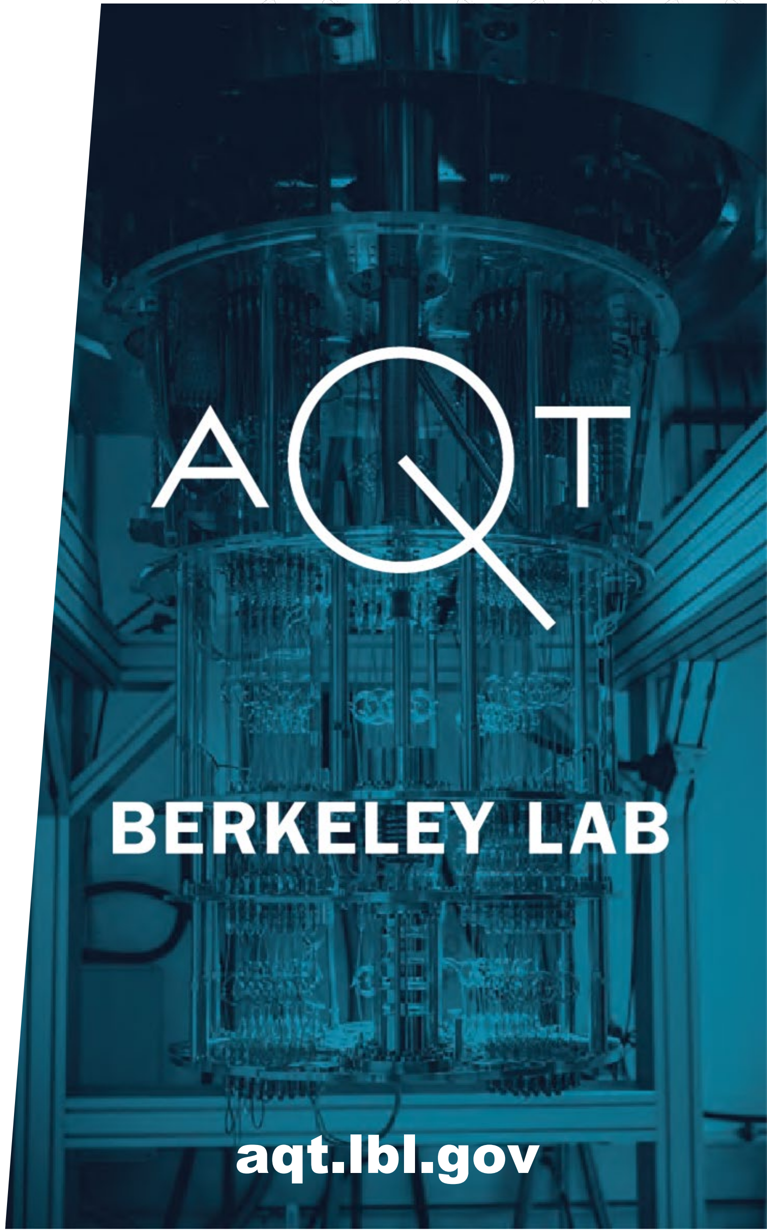

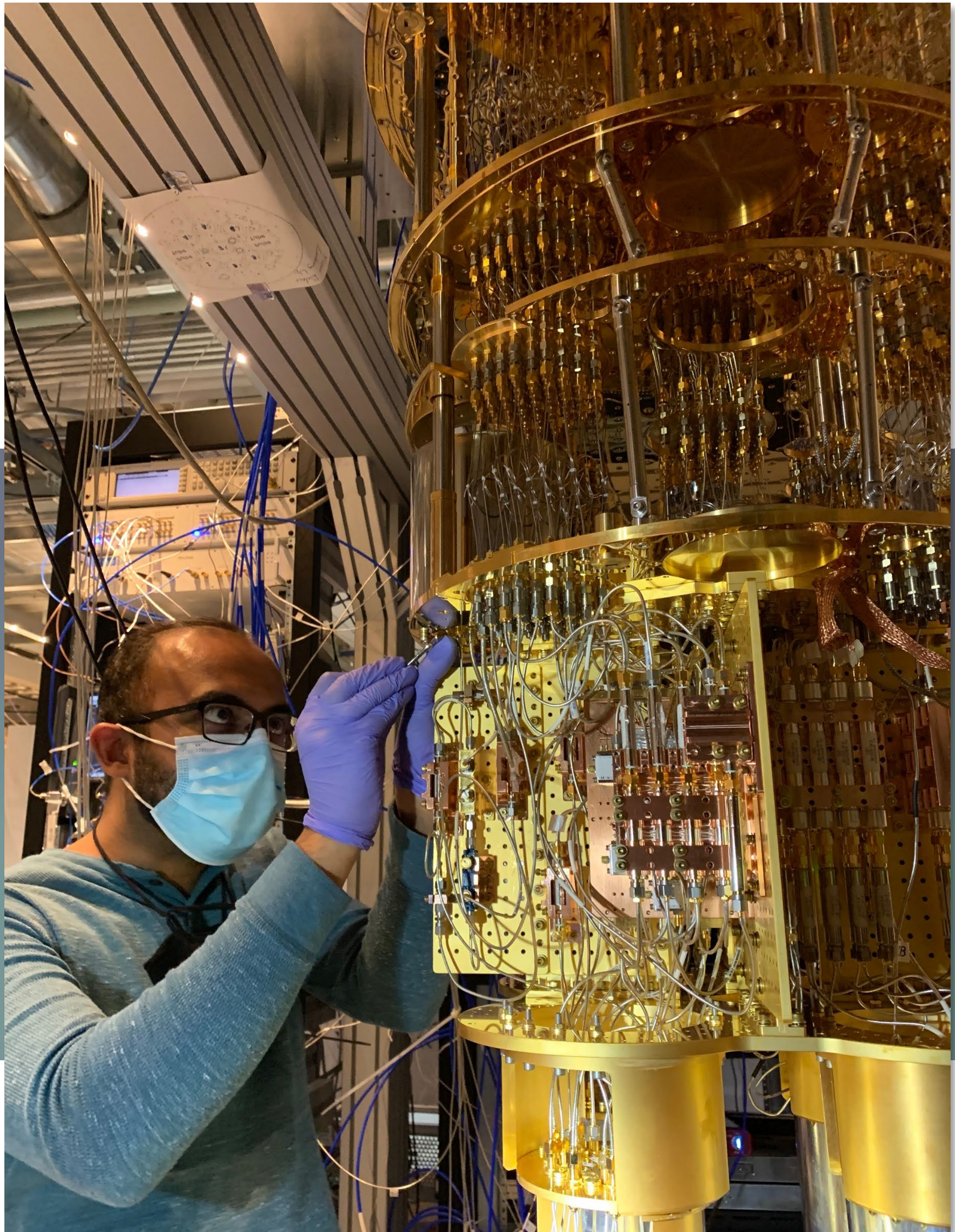

Mission

Serve as an advanced superconducting platform for quantum computation and foster deep research collaborations with users selected through an open, competitive proposal process to create synergies with other resources available to the researcher community.

The Key Pieces

Unique Quantum Platform

A state-of-the art open platform based on superconducting circuits for the scientific exploration of quantum computing, including quantum circuit fidelity, control/compilation, and processor architecture.

Deep User Collaborations

A highly-qualified team assists and partners in the development, execution, and optimization of short- and long-term scientific projects.

Broad Exploration of Technology

AQT deploys an evolving suite of circuits, controls, classical hardware, and algorithms developed at LBNL and via commercial partnerships.

Developing Future QIS Experts

An ideal platform for training the next generation of scientists and engineers on cutting-edge hardware and real-world problems.

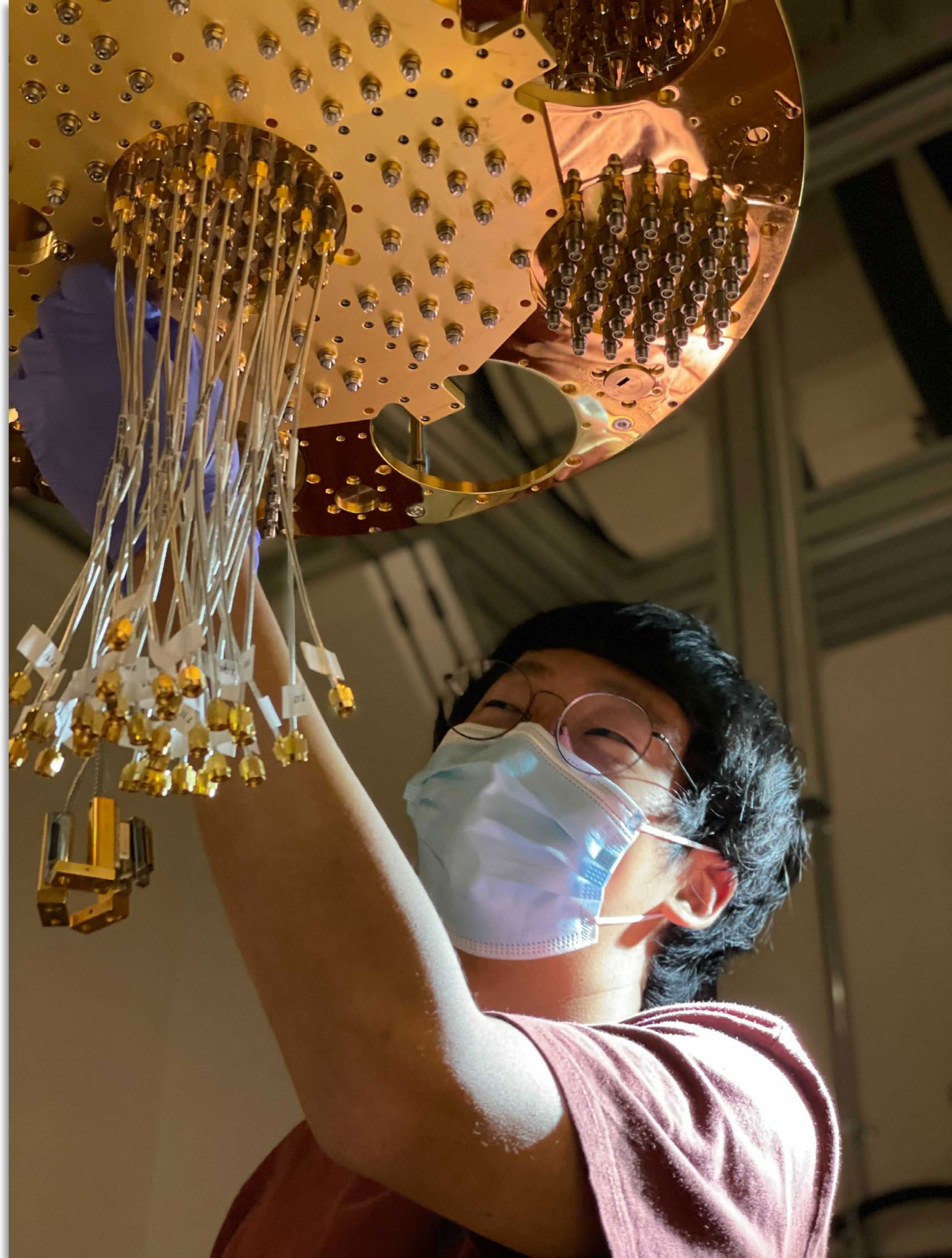

AQT Processor Range

Exploring the breadth of superconducting quantum technology

Highly Coherent
Hardware Efficient

Highly Connected
Reconfigurable

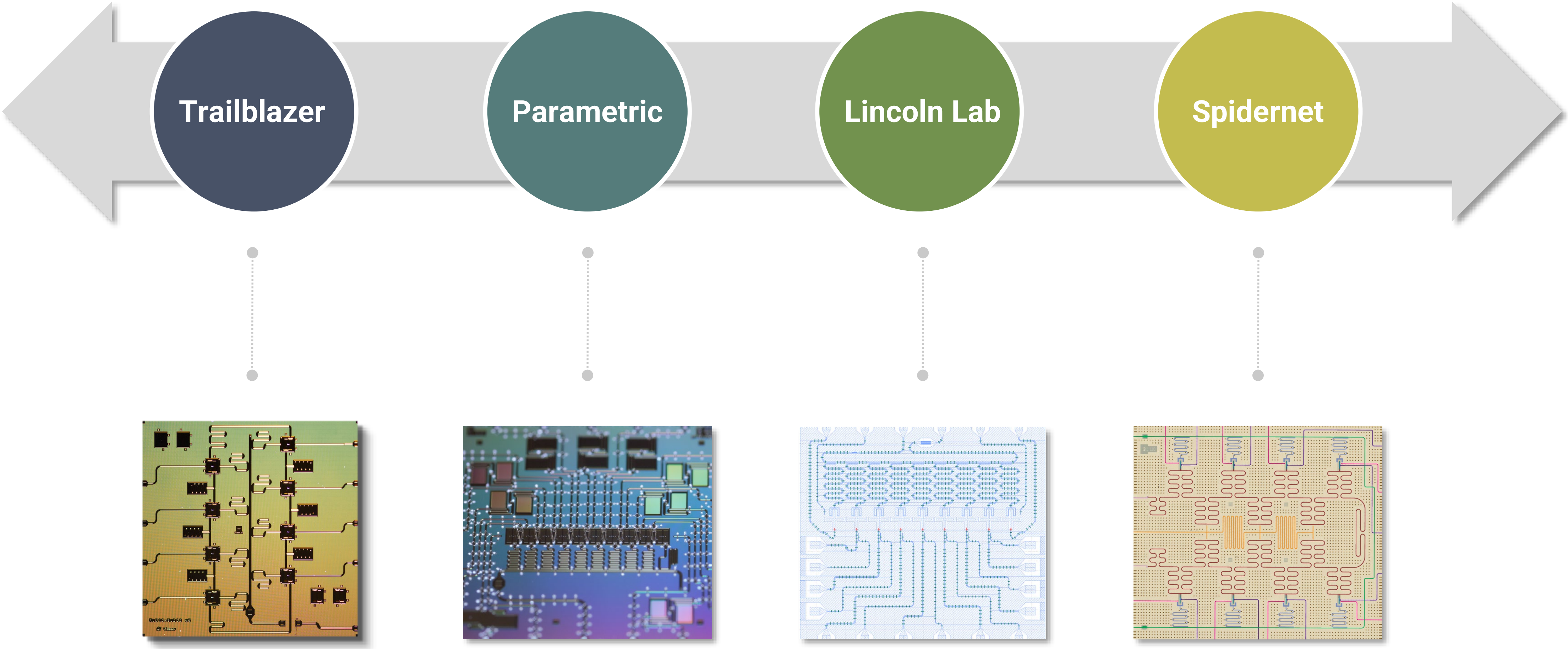

High-coherence Transmon qubits

Eight fixed-frequency qubits

Coherence times: $T_1 \sim 50 - 150\ \mu s$, $T_2 \sim 50 - 150\ \mu s$

Qubit frequencies: $5 - 6$ GHz, Anharmonicities: $250 - 270$ MHz

Multiplexed Dispersive Readout

Enabled by Travelling-Wave Parametric Amplification (TWPA)

Three-state readout fidelities: $\mathrm{P}(0|0) \sim 99.6\% - 99.8\%$,

$\mathrm{P}(1|1) \sim 97\% - 99\%$, $\mathrm{P}(2|2) \sim 94\% - 97\%$

All-microwave Quantum Control

Universal single-qubit gates (60 ns), fidelity: $99.7\% - 99.95\%$

Two-qubit differential AC-Stark CZ gates[1] (200 ns): $99\% - 99.5\%$

Nearest-neighbor resonator-mediated connectivity in a ring

Novel Capabilities

Three-qubit iToffoli gates[2] (350 ns): 98.26%

Two-*qutrit* CZ gates: 97.3%

Programmable Heisenberg interactions, iSWAP gates[3]: 99.3%

[1] Mitchell PRL (2021), [2] Kim Nat. Phys. (2022), [3] Nguyen arXiv:2211.10383 (2022)

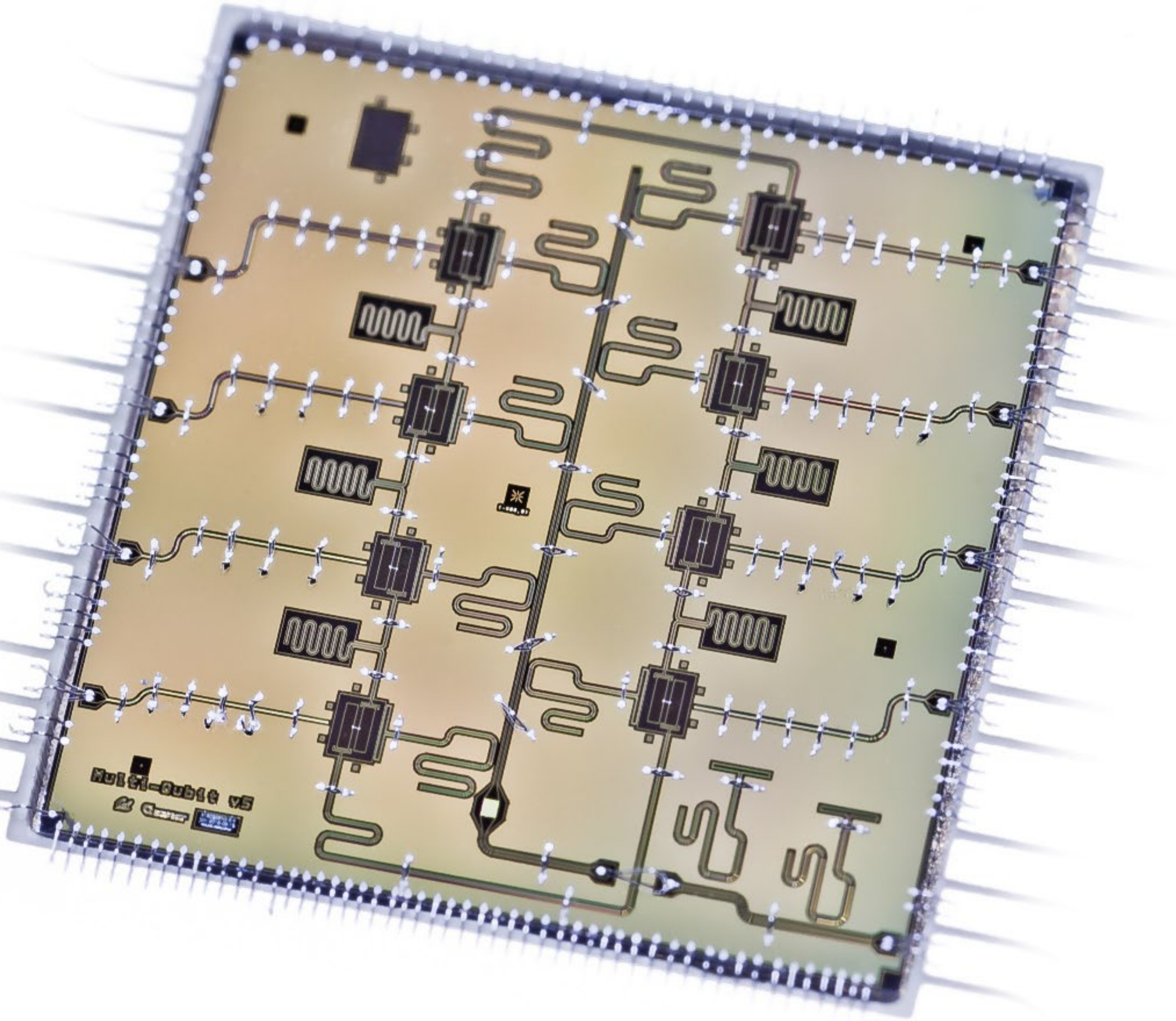

Trailblazer

High Coherence, Efficient Control

High-coherence Transmon qubits

Eight fixed-frequency qubits

Coherence times: $T_1 \sim 50 - 150\ \mu s$, $T_2 \sim 50 - 150\ \mu s$

Qubit frequencies: $5 - 6$ GHz, Anharmonicities: $250 - 270$ MHz

Multiplexed Dispersive Readout

Enabled by Travelling-Wave Parametric Amplification (TWPA)

Three-state readout fidelities: $\mathrm{P}(0|0) \sim 99.6\% - 99.8\%$,

$\mathrm{P}(1|1) \sim 97\% - 99\%$, $\mathrm{P}(2|2) \sim 94\% - 97\%$

All-microwave Quantum Control

Universal single-qubit gates (60 ns), fidelity: $99.7\% - 99.95\%$

Two-qubit differential AC-Stark CZ gates[1] (200 ns): $99\% - 99.5\%$

Nearest-neighbor resonator-mediated connectivity in a ring

Novel Capabilities

Three-qubit iToffoli gates[2] (350 ns): 98.26%

Two-*qutrit* CZ gates: 97.3%

Programmable Heisenberg interactions, iSWAP gates[3]: 99.3%

[1]Mitchell PRL (2021), [2]Kim Nat. Phys. (2022), [3]Nguyen arXiv:2211.10383 (2022)

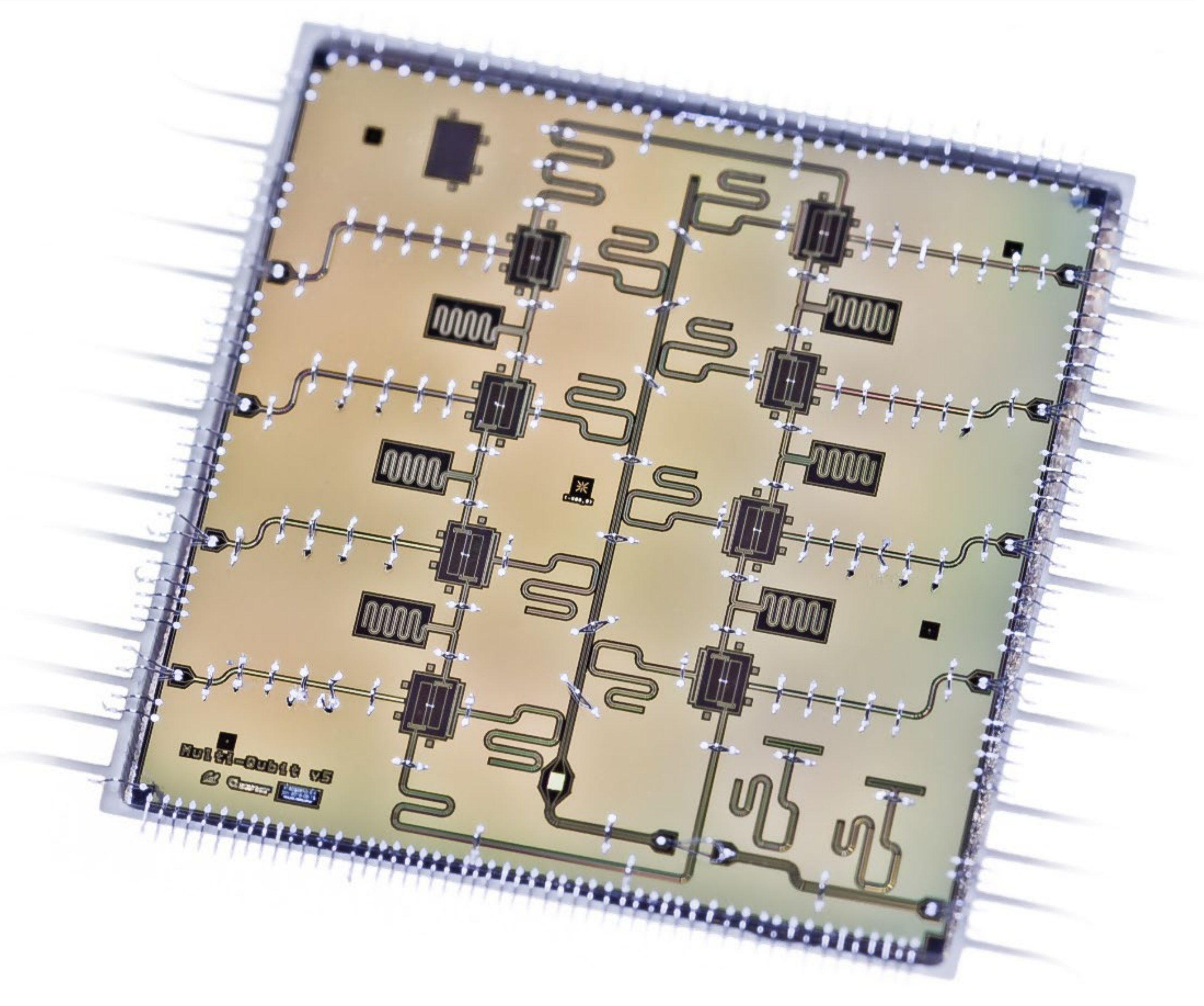

Trailblazer

High Coherence, Efficient Control

What is a superconducting qutrit?

$|\psi\rangle = \alpha|0\rangle + \beta|1\rangle + \gamma|2\rangle$, qutrit

$|\psi\rangle = \alpha|0\rangle + \beta|1\rangle$ qubit

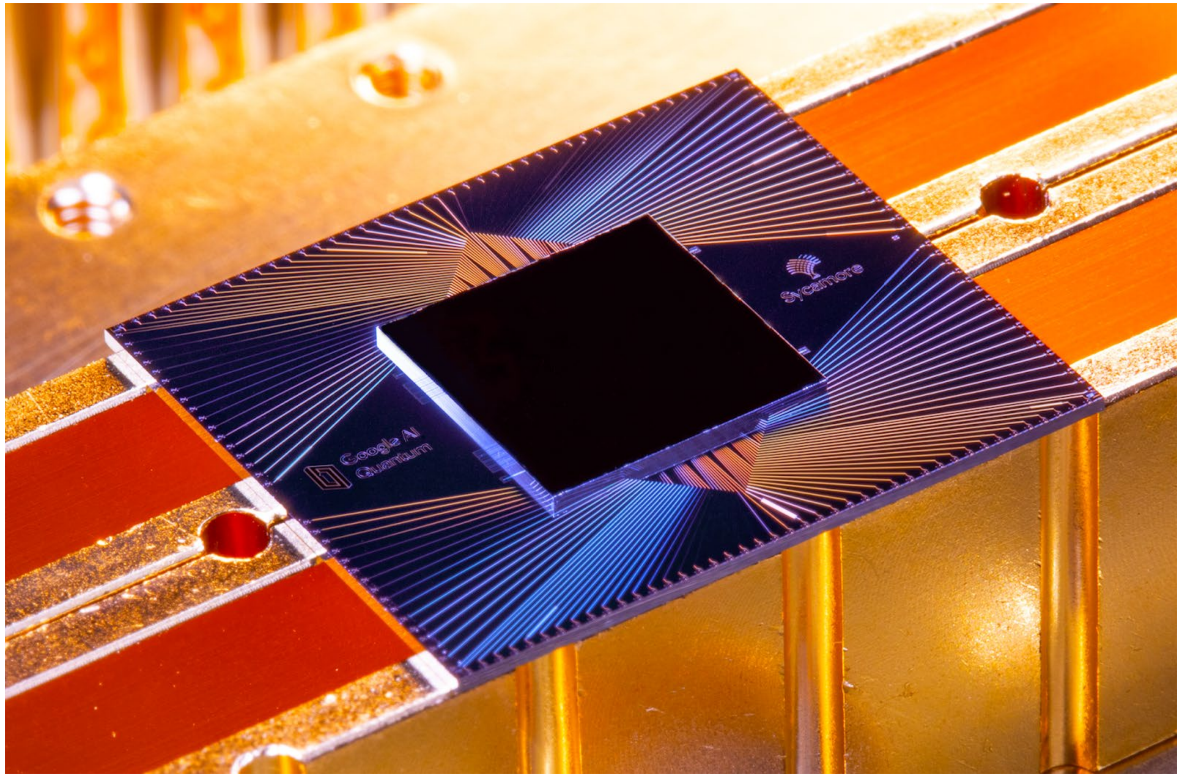

Google sycamore processor

$$\mathrm{H}_{\mathrm{Transmon}} \approx \left(\sqrt{8E_cE_J} - \frac{E_C}{2}\right)a^{\dagger}a - \frac{E_C}{2}(a^{\dagger}a)^2$$

J. Koch *et al.* Phys. Rev. A **76**, 042319 (2007)

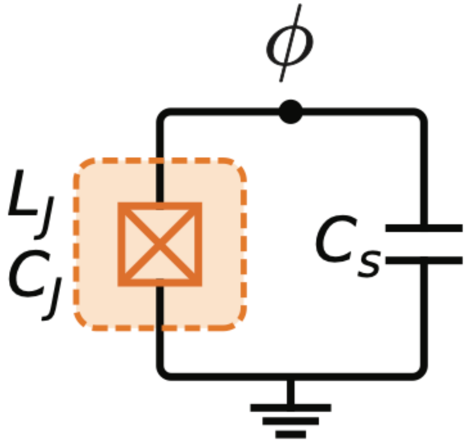

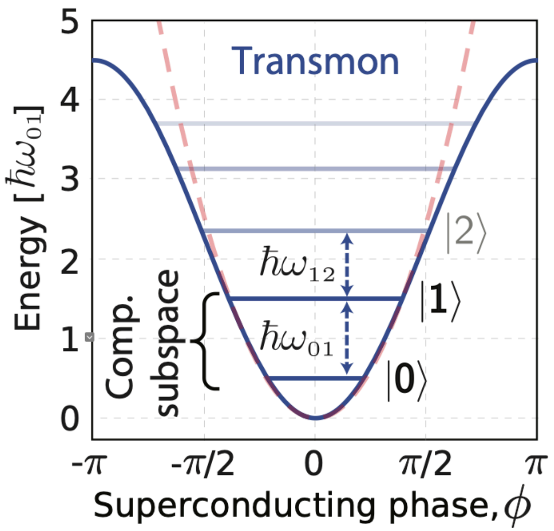

Krantz et al. Applied Physics Reviews **6**, 021318 (2019)

Superconducting qubits are inherently multilevel systems

Improved coherence enables qutrit realization

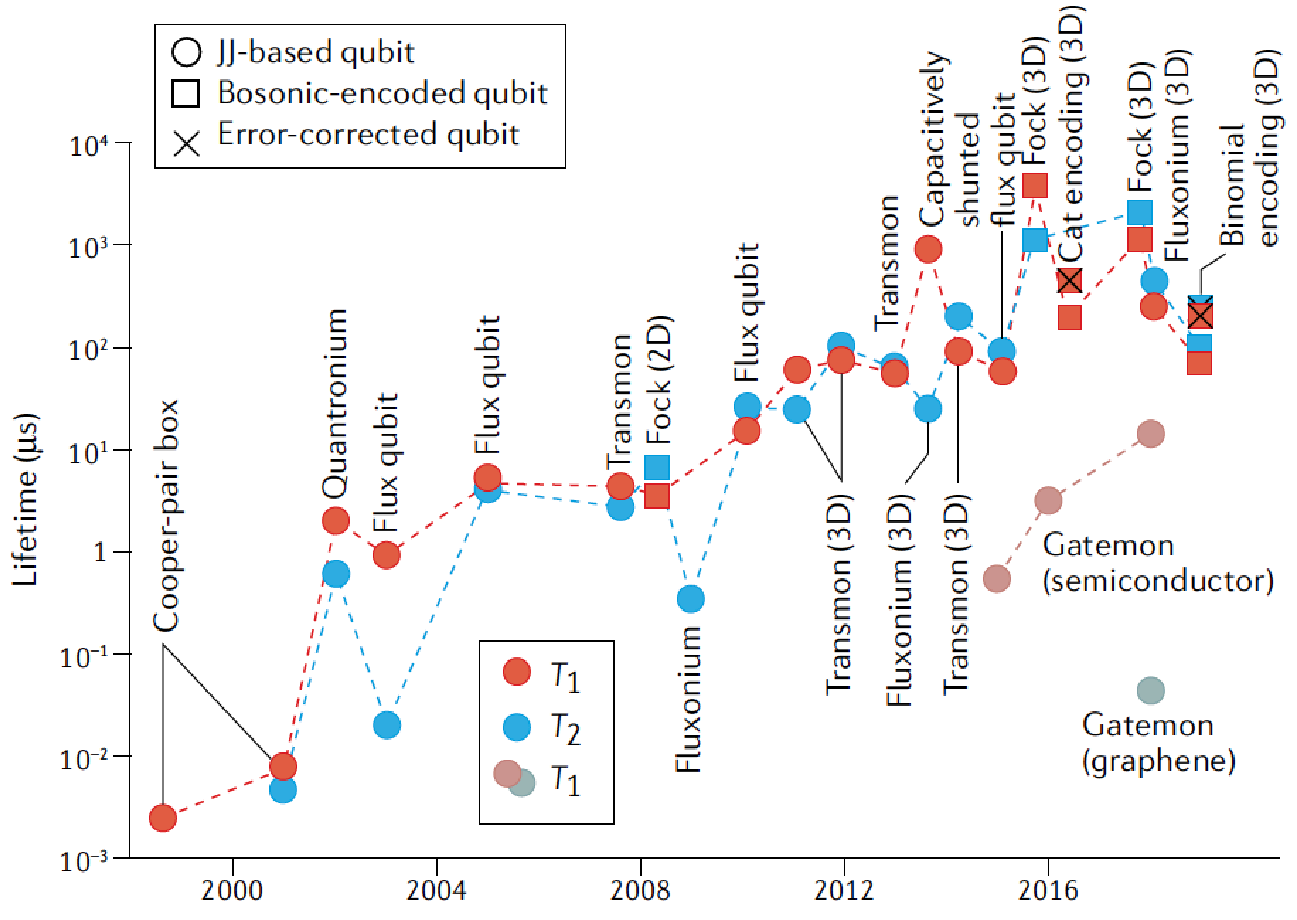

I. Siddiqi Nature Review Materials. **6**, 875-891 (2021)

$$\epsilon_m \approx (-1)^m E_C \frac{2^{4m+5}}{m!} \sqrt{\frac{2}{\pi}} \left(\frac{E_J}{2E_C}\right)^{\frac{m}{2}+\frac{3}{4}} e^{-\sqrt{8E_J/E_C}},$$

M. S. Blok *et al.* Phys. Rev. X **11**, 021010 (2021),

	Q3	Q4
Qubit freq. (GHz)	5.436	5.327
Anharm. (MHz)	-260.20	-262.94
T_1^{01} (μs)	125(37)	78(16)
T_1^{12} (μs)	63(9)	47(5)
T_{2e}^{01} (μs)	190(28)	138(25)
T_{2e}^{12} (μs)	61(13)	45(7)
T_{2e}^{02} (μs)	75(19)	62(6)
T_{2r}^{01} (μs)	114(47)	99(24)
T_{2r}^{12} (μs)	17(8)	17(9)
T_{2r}^{02} (μs)	20(16)	21(9)

Goss *et al.* Nature Communications **13**, 7481 (2022),

What can we do with noisy qutrits?

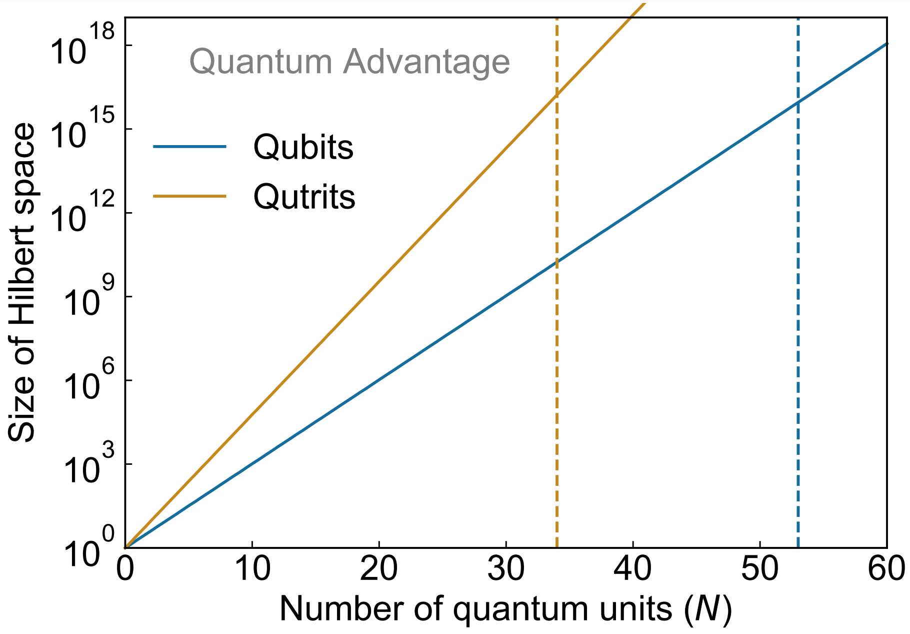

$$|\Psi\rangle = |\psi_i\rangle^{\otimes_{i=1,\dots,N}}, \qquad ||\Psi\rangle| = 3^N$$

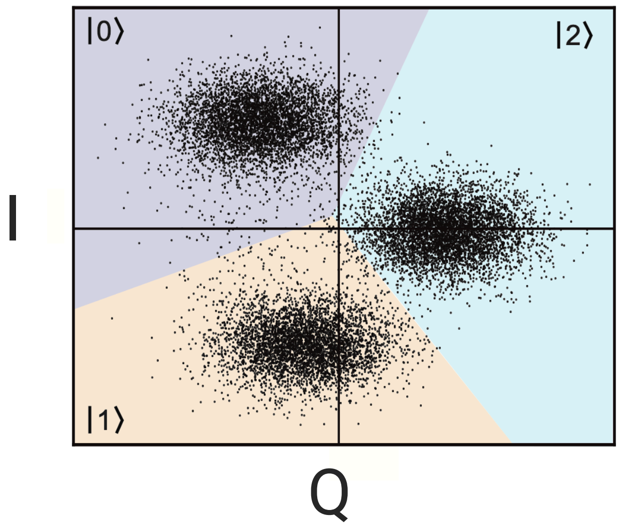

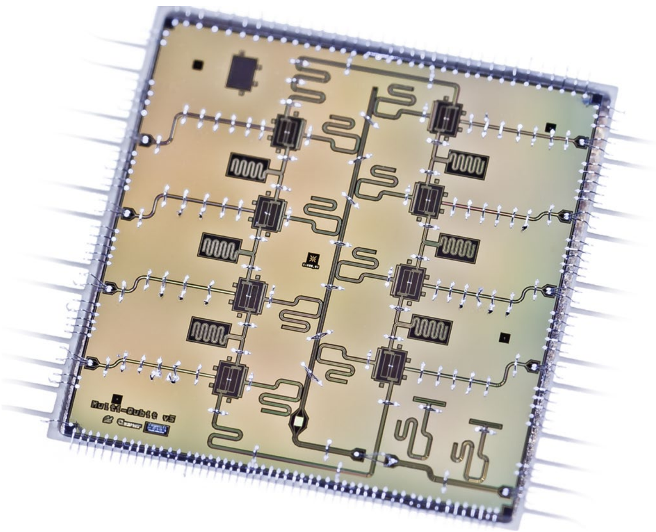

What can we do with noisy qutrits?

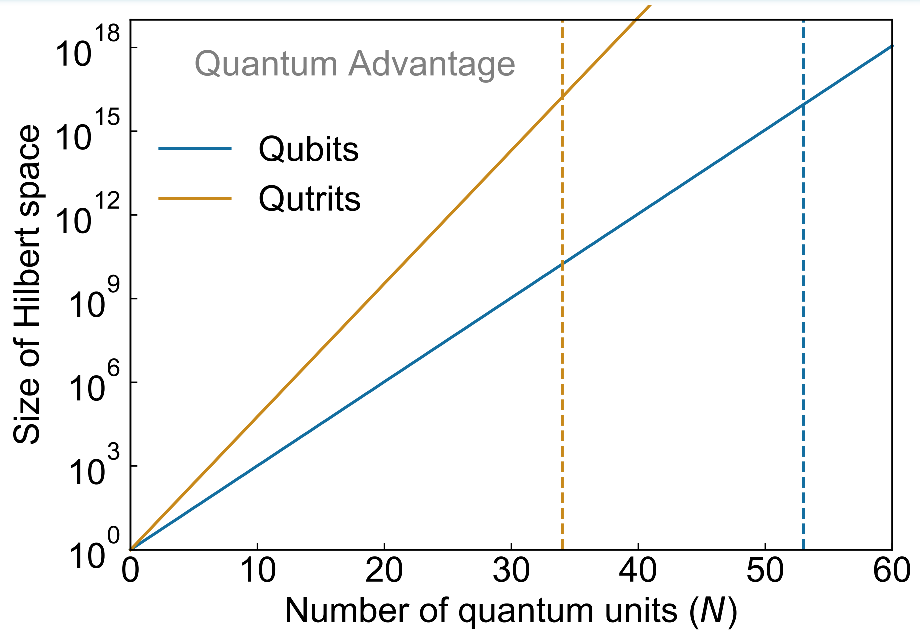

$$|\Psi\rangle = |\psi_i\rangle^{\otimes_{i=1,\dots,N}} , \qquad ||\Psi\rangle| = 3^N$$

- Larger Hilbert Space: 35 transmon device yields increase of order 10^6 → regime of quantum advantage
  - Arute *et al.* Nature. **574**, 505–510 (2019)

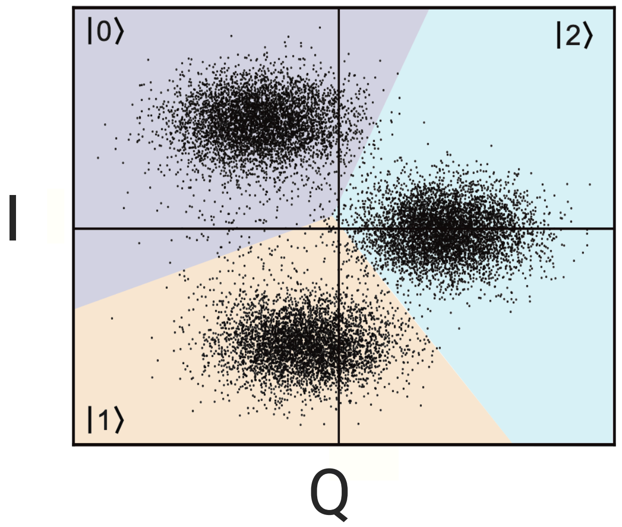

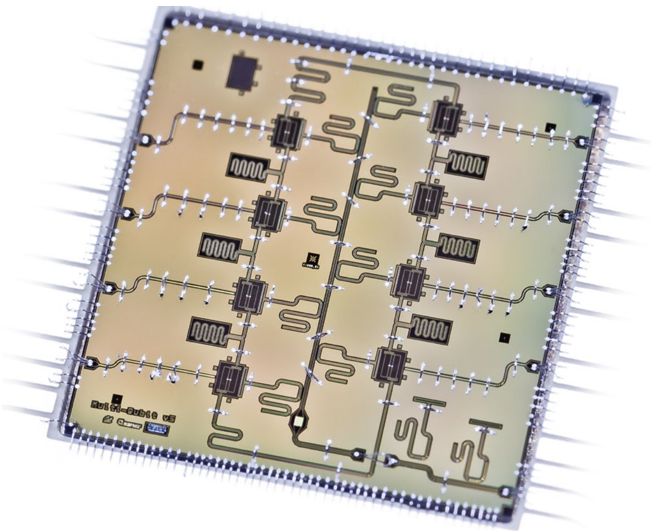

What can we do with noisy qutrits?

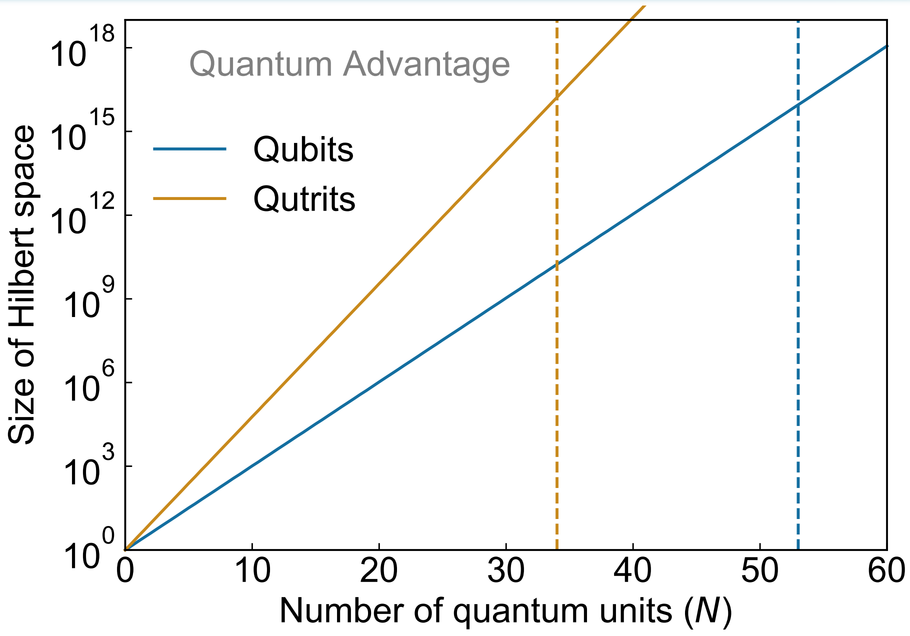

$$|\Psi\rangle = |\psi_i\rangle^{\otimes_{i=1,\dots,N}}, \qquad ||\Psi\rangle| = 3^N$$

- Larger Hilbert Space: 35 transmon device yields increase of order 10^6 → regime of quantum advantage
  - Arute *et al.* Nature. **574**, 505–510 (2019)
- Resource efficient, noise resilient for certain quantum simulations
  - M. S. Blok *et al.* Phys. Rev. X **11**, 021010 (2021), Gustafson, arXiv:2201.0456 (2022)

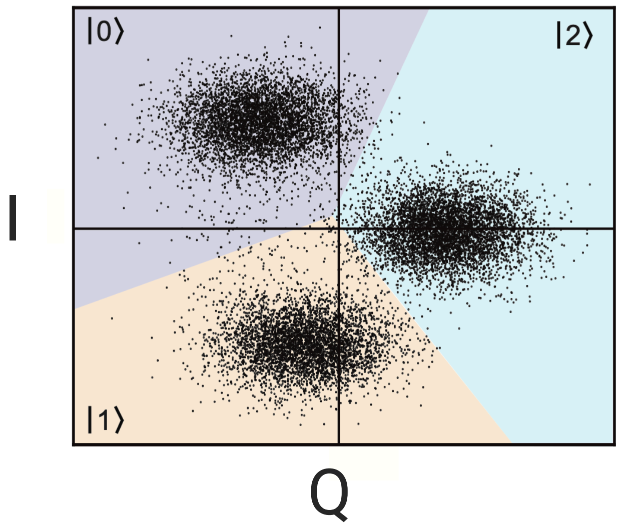

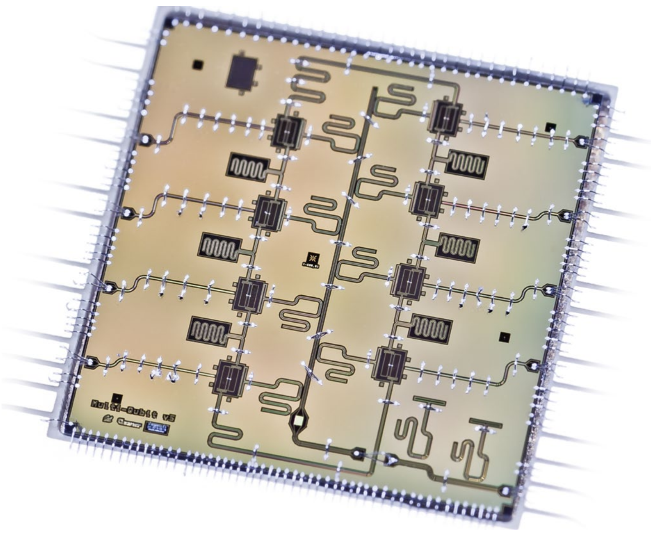

What can we do with noisy qutrits?

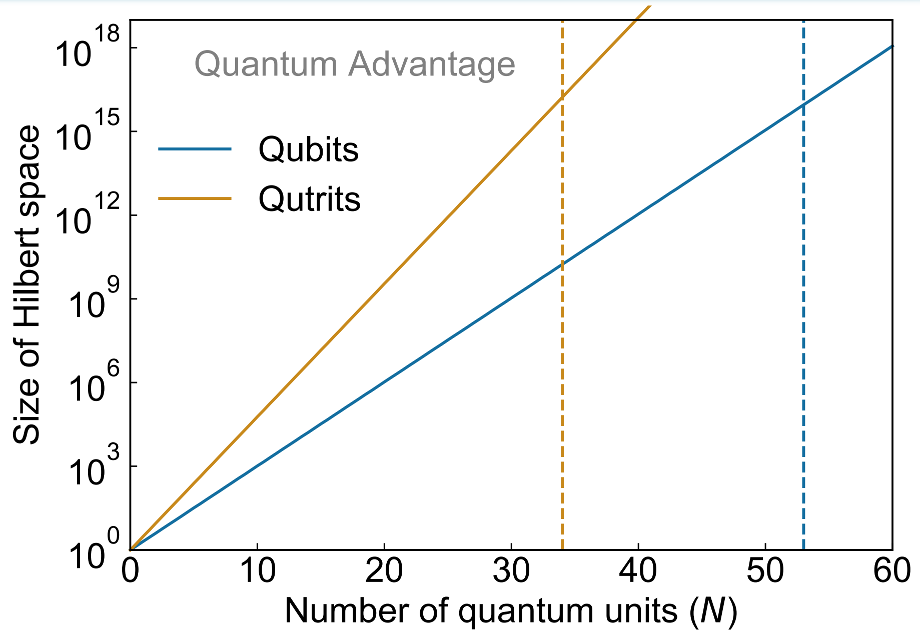

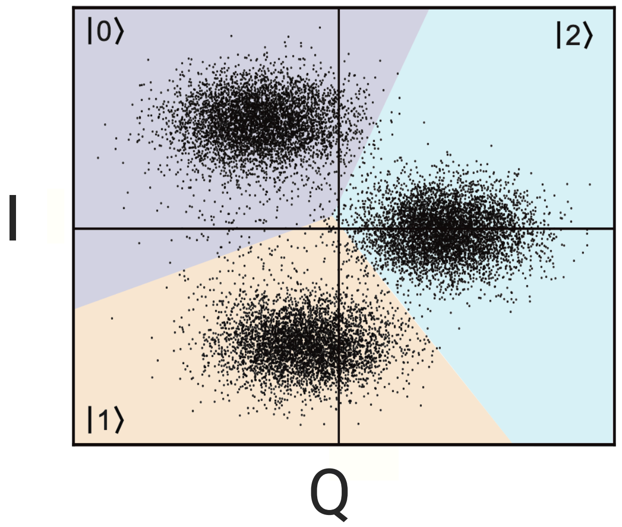

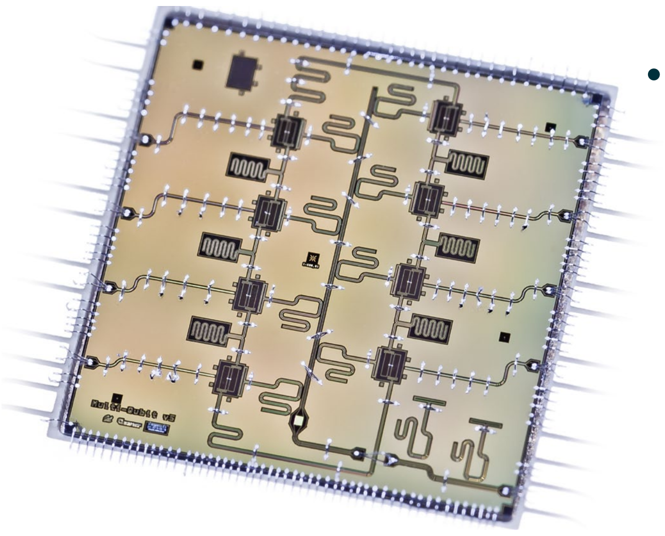

$$|\Psi\rangle = |\psi_i\rangle^{\otimes_{i=1,\dots,N}}, \qquad ||\Psi\rangle| = 3^N$$

- Larger Hilbert Space: 35 transmon device yields increase of order 10^6 → regime of quantum advantage
  - Arute *et al.* Nature. **574**, 505–510 (2019)
- Resource efficient, noise resilient for certain quantum simulations
  - M. S. Blok *et al.* Phys. Rev. X **11**, 021010 (2021), Gustafson, arXiv:2201.0456 (2022)
- Robust and resource efficient Quantum Error Correction for logical qutrits
  - Muralidharan *et al.* 2017 *New J. Phys.* **19** 013026

What can we do with noisy qutrits?

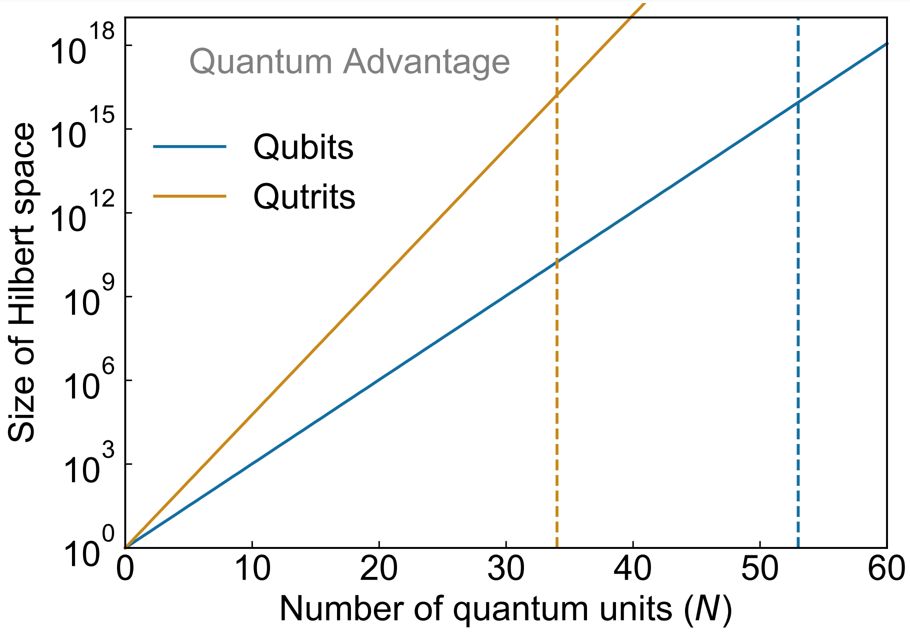

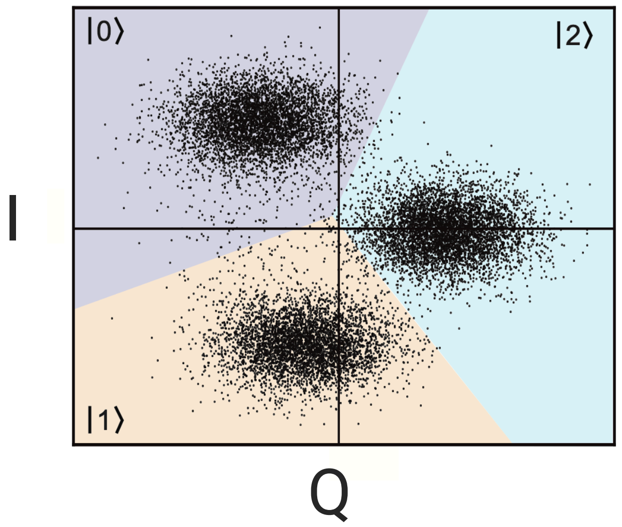

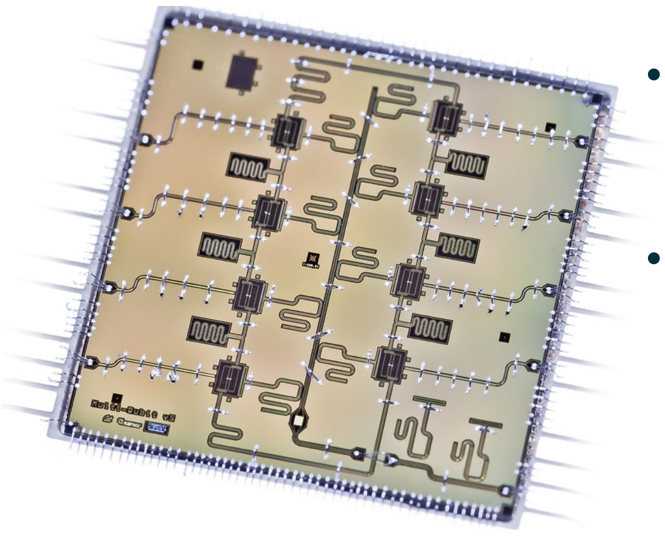

$$|\Psi\rangle = |\psi_i\rangle^{\otimes_{i=1,\dots,N}}, \qquad ||\Psi\rangle| = 3^N$$

- Larger Hilbert Space: 35 transmon device yields increase of order 10^6 → regime of quantum advantage
  - Arute *et al.* Nature. **574**, 505–510 (2019)
- Resource efficient, noise resilient for certain quantum simulations
  - M. S. Blok *et al.* Phys. Rev. X **11**, 021010 (2021), Gustafson, arXiv:2201.0456 (2022)
- Robust and resource efficient Quantum Error Correction for logical qutrits
  - Muralidharan *et al.* 2017 *New J. Phys.* **19** 013026
- **However:** Requires a scalable, high-fidelity entangling gate

Qutrit logic crash course

Paulis (qubit) → Weyls (qutrit)

$X = \sum_{n\in\mathbb{Z}_3} |n+1\rangle\langle n| \quad Z\,|n\rangle = \omega^n\,|n\rangle,\ \ \omega = e^{2\pi i/3} \quad H = \frac{1}{\sqrt{d}}\sum_{i,j}\omega^{ij}|i\rangle\langle j|$

$\{W_{x,z} = X^x Z^z, x, z \in \mathbb{Z}_3\}$

Qutrit logic crash course

Paulis (qubit) → Weyls (qutrit)

$X = \sum_{n \in \mathbb{Z}_3} |n+1\rangle\langle n|$ $\quad Z\,|n\rangle = \omega^n\,|n\rangle,\ \omega = e^{2\pi i/3}$ $\quad H = \frac{1}{\sqrt{d}} \sum_{i,j} \omega^{ij} |i\rangle\langle j|$

$\{W_{x,z} = X^x Z^z, x, z \in \mathbb{Z}_3\}$

$$CZ = \sum_{n=1}^{3} |n\rangle\langle n| \otimes Z^n$$

Qutrit logic crash course

Paulis (qubit) → Weyls (qutrit)

$X = \sum_{n \in \mathbb{Z}_3} |n+1\rangle\langle n|$ $\quad Z|n\rangle = \omega^n |n\rangle, \ \omega = e^{2\pi i/3}$ $\quad H = \frac{1}{\sqrt{d}} \sum_{i,j} \omega^{ij} |i\rangle\langle j|$

$\{W_{x,z} = X^x Z^z, x, z \in \mathbb{Z}_3\}$

$CZ = \sum_{n=1}^{3} |n\rangle\langle n| \otimes Z^n$ ⟶ $\text{CSUM} = (I \otimes H^\dagger) CZ (I \otimes H)$

Qutrit logic crash course

Paulis (qubit) → Weyls (qutrit)

$$X = \sum_{n\in\mathbb{Z}_3} |n+1\rangle\langle n| \qquad Z\,|n\rangle = \omega^n\,|n\rangle,\ \ \omega = e^{2\pi i/3} \qquad H = \frac{1}{\sqrt{d}}\sum_{i,j}\omega^{ij}|i\rangle\langle j|$$

$$\{W_{x,z} = X^x Z^z, x, z \in \mathbb{Z}_3\}$$

Generalization of the CNOT:

$\mathrm{CSUM}|i,j\rangle = |i, i+j \bmod 3\rangle$

$$CZ = \sum_{n=1}^{3} |n\rangle\langle n| \otimes Z^n \longrightarrow \mathrm{CSUM} = (I\otimes H^\dagger)CZ(I\otimes H) \longleftrightarrow$$

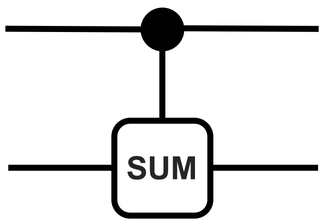

Qutrit logic crash course

Paulis (qubit) → Weyls (qutrit)

$$X = \sum_{n\in\mathbb{Z}_3} |n+1\rangle\langle n| \quad Z|n\rangle = \omega^n |n\rangle,\ \omega = e^{2\pi i/3} \quad H = \frac{1}{\sqrt{d}} \sum_{i,j} \omega^{ij} |i\rangle\langle j|$$

$$\{W_{x,z} = X^x Z^z, x, z \in \mathbb{Z}_3\}$$

Generalization of the CNOT:

$\mathrm{CSUM}|i,j\rangle = |i, i+j \bmod 3\rangle$

$$CZ = \sum_{n=1}^{3} |n\rangle\langle n| \otimes Z^n \longrightarrow \mathrm{CSUM} = (I \otimes H^\dagger) CZ (I \otimes H) \longleftrightarrow$$

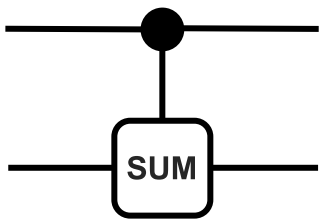

D = 9 → larger Hilbert space than 3 qubit Toffoli gate

Single qutrit control

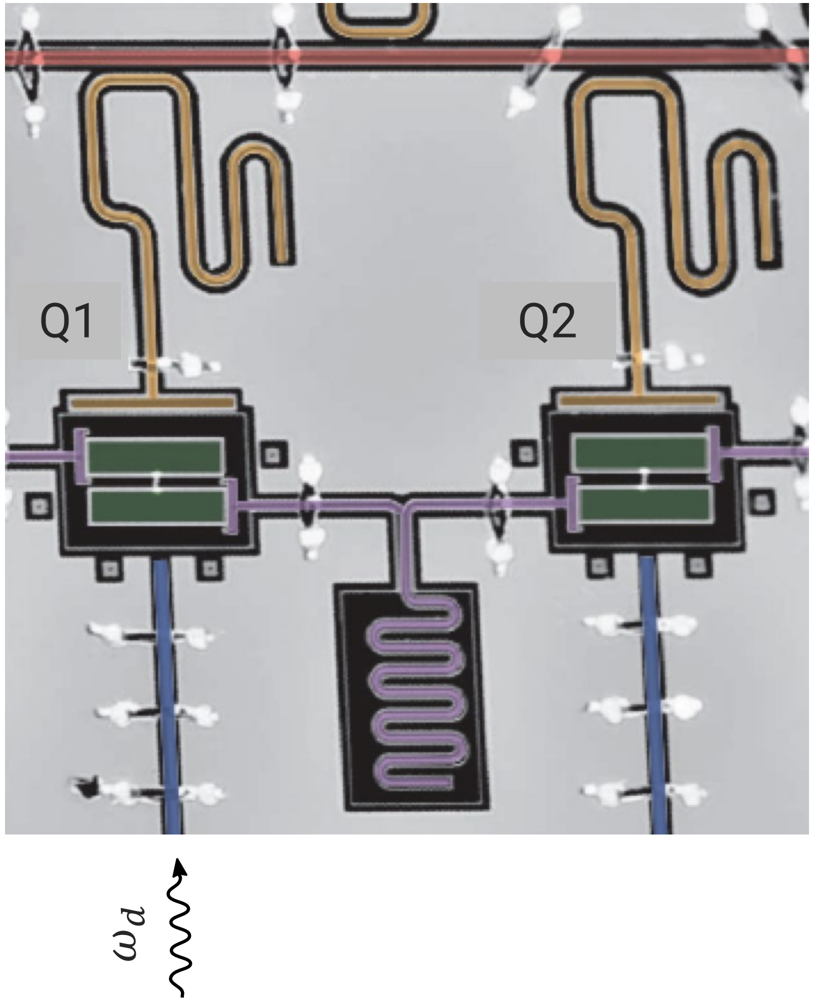

Single qutrit gates: U(3) Decomposition via 6 native subspace pulses, virtual Z gates

Morvan *et al.* Phys. Rev. Lett. **126**, 210504, (2021)

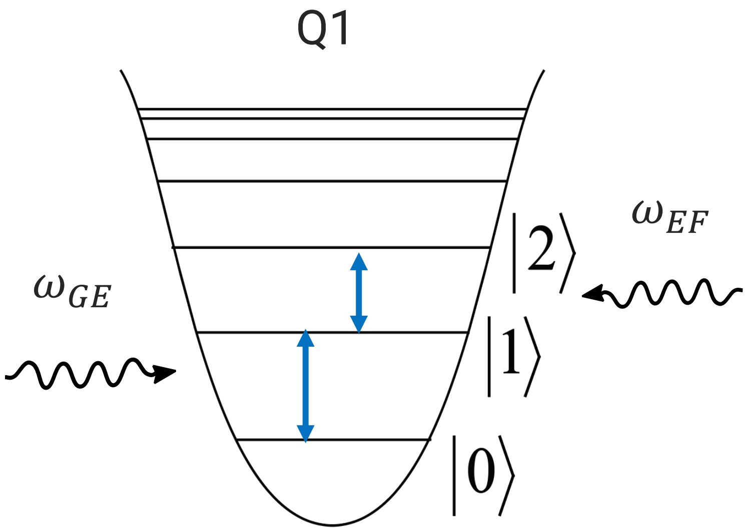

$\{G = |0\rangle, \;\; E = |1\rangle, \;\; F = |2\rangle\}$

Subspace Rabi oscillations + virtual Z gates enables universal single qutrit control

Recipe for high-fidelity qutrit entanglement

Recipe for high-fidelity qutrit entanglement

Microwave-activated entangling interaction for fixed frequency qutrits
Mitchell *et al.* Phys. Rev. Lett. **127**, 200502, (2021)

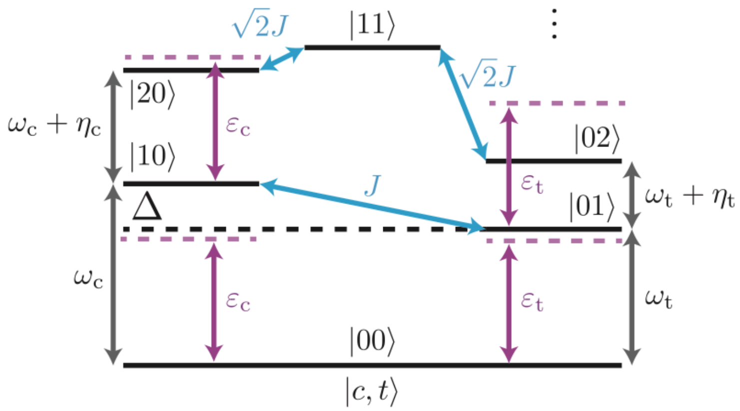

Recipe for high-fidelity qutrit entanglement

Microwave-activated entangling interaction for fixed frequency qutrits
Mitchell *et al.* Phys. Rev. Lett. **127**, 200502, (2021)

Leverage this interaction → Maximally entangling Qutrit C-Phase gate

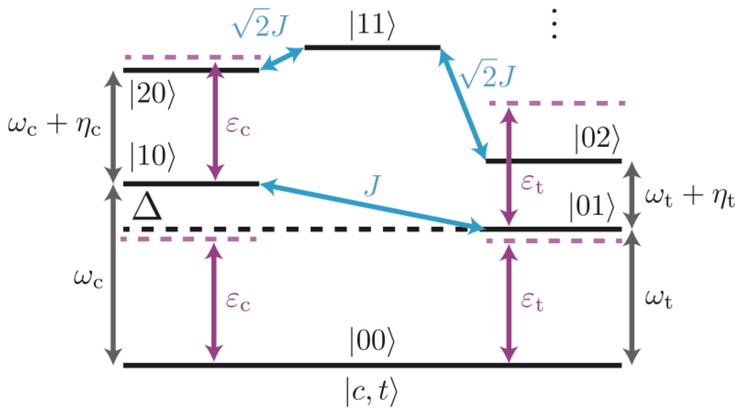

Recipe for high-fidelity qutrit entanglement

Microwave-activated entangling interaction for fixed frequency qutrits
Mitchell *et al.* Phys. Rev. Lett. **127**, 200502, (2021)

Leverage this interaction → Maximally entangling Qutrit C-Phase gate

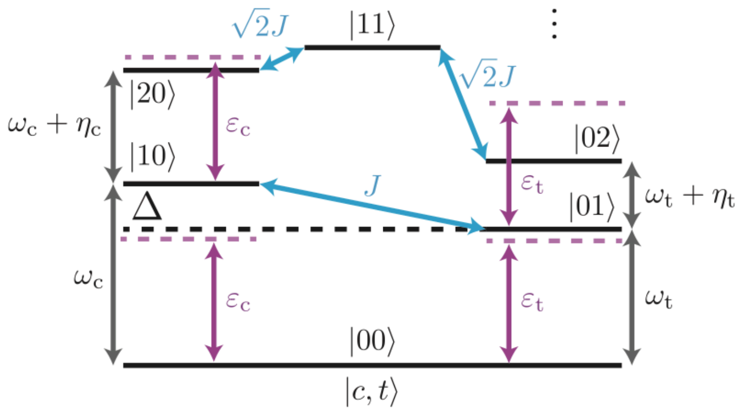

Characterize and Benchmark Gate

Qutrit Randomized Benchmarking and Cycle Benchmarking experimentally demonstrated, 99.7% single qutrit gates
Morvan *et al.* Phys. Rev. Lett. **126**, 210504, (2021)

CSUM with $\mathcal{F} = 0.889$ demonstrated using static interaction
M. S. Blok *et al.* Phys. Rev. X **11**, 021010 (2021)

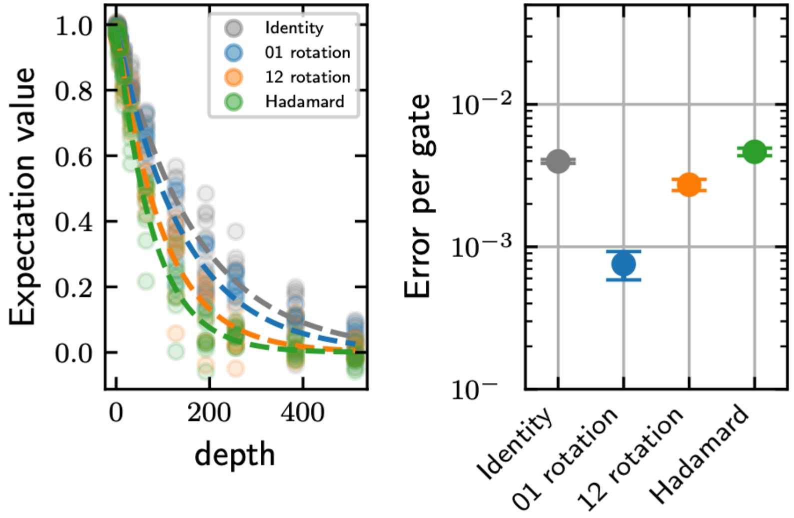

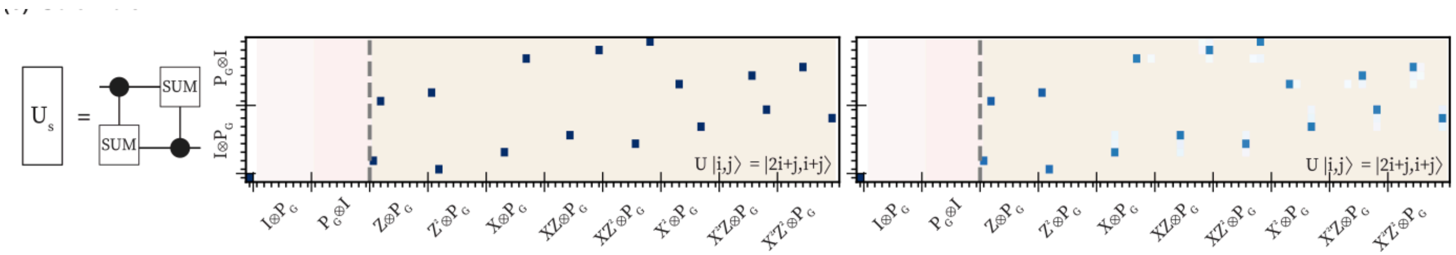

Qutrit cross-Kerr entanglement

2 qutrit Hamiltonian

$$H = \sum_{i=a,b} \omega_i a_i^\dagger a_i + \frac{\eta_i}{2} a_i^\dagger a_i^\dagger a_i a_i + J(a_C^\dagger a_T + a_C a_T^\dagger)$$

Fixed-frequency, fixed-coupling architecture

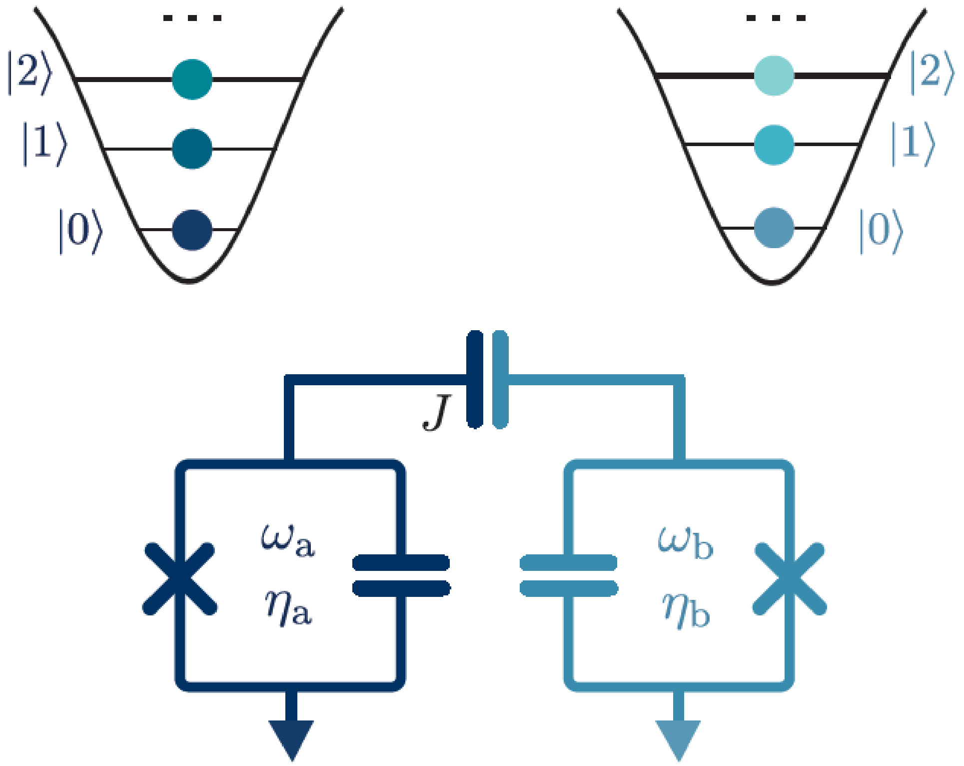

Qutrit cross-Kerr entanglement

2 qutrit Hamiltonian

$$H = \sum_{i=a,b} \omega_i a_i^\dagger a_i + \frac{\eta_i}{2} a_i^\dagger a_i^\dagger a_i a_i + J(a_C^\dagger a_T + a_C a_T^\dagger)$$

Qutrit Kerr Coupling Hamiltonian

$$H_{\mathrm{Kerr}} = \alpha_{11}|11\rangle\langle 11| + \alpha_{12}|12\rangle\langle 12| + \alpha_{21}|21\rangle\langle 21| + \alpha_{22}|22\rangle|\langle 22|,$$

$$\alpha_{ij} = (E_{ij} - E_{i0}) - (E_{0j} - E_{00})$$

M. S. Blok *et al.* Phys. Rev. X **11**, 021010 (2021)

Fixed-frequency, fixed-coupling architecture

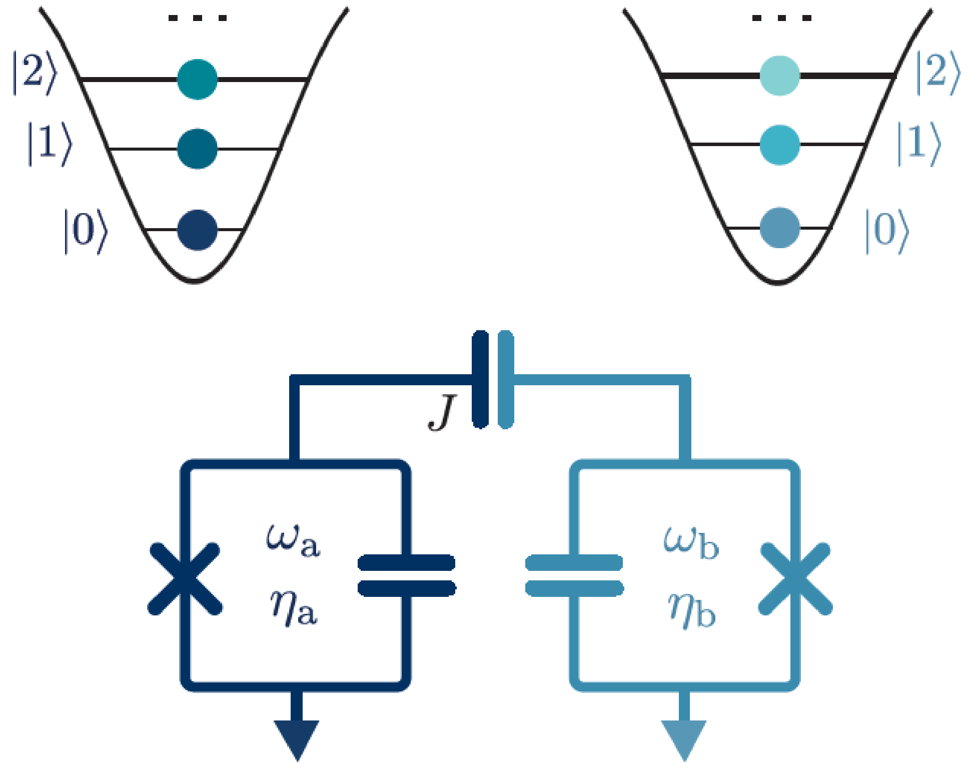

Qutrit cross-Kerr entanglement

Fixed-frequency, fixed-coupling architecture

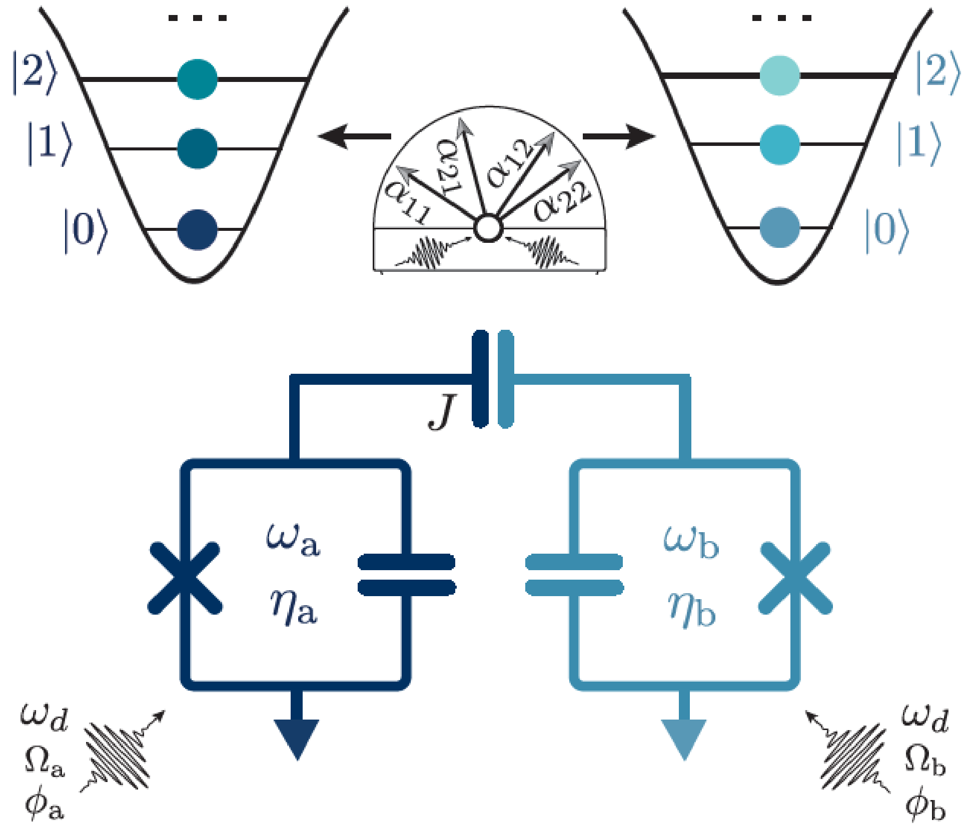

2 qutrit Hamiltonian

$$H = \sum_{i=a,b} \omega_i a_i^\dagger a_i + \frac{\eta_i}{2} a_i^\dagger a_i^\dagger a_i a_i + J(a_C^\dagger a_T + a_C a_T^\dagger)$$

Qutrit Kerr Coupling Hamiltonian

$$H_{\mathrm{Kerr}} = \alpha_{11}|11\rangle\langle 11| + \alpha_{12}|12\rangle\langle 12| + \alpha_{21}|21\rangle\langle 21| + \alpha_{22}|22\rangle|\langle 22|,$$

$$\alpha_{ij} = (E_{ij} - E_{i0}) - (E_{0j} - E_{00})$$

M. S. Blok *et al.* Phys. Rev. X **11**, 021010 (2021)

Simultaneous Drive With Differential AC Stark Shift

$$H = \sum_{i=a,b} [(\omega_i - \omega_d) a_i^\dagger a_i + \frac{\eta_i}{2} a_i^\dagger a_i^\dagger a_i a_i + \Omega_i \left(e^{i\phi_i} a_i + e^{-i\phi_i} a_i^\dagger\right) + J(a_C^\dagger a_T + a_C a_T^\dagger)]$$

$$\alpha_{ij}(\omega_d, \Omega_{a,b}, \phi_{a,b})$$

Characterizing the driven cross-Kerr

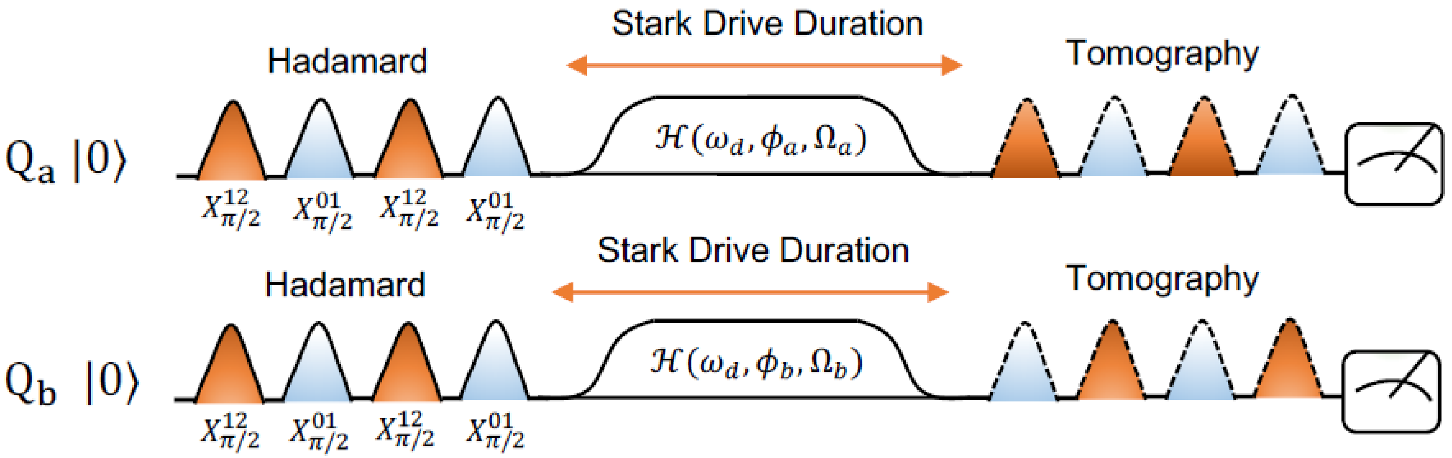

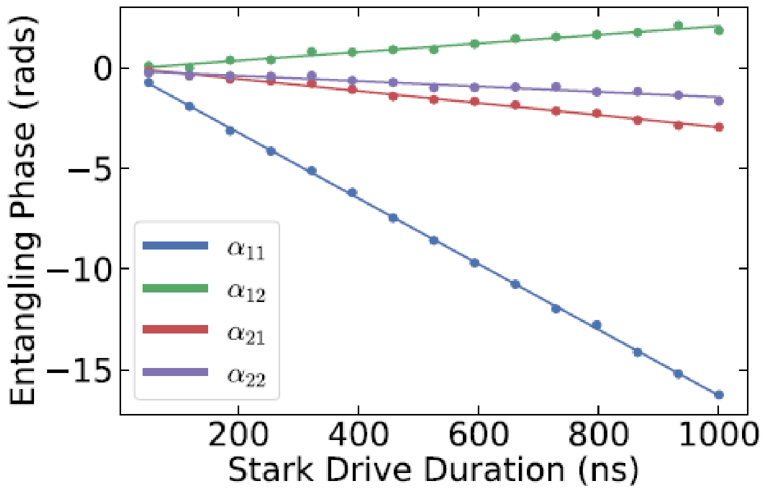

Characterizing the driven cross-Kerr

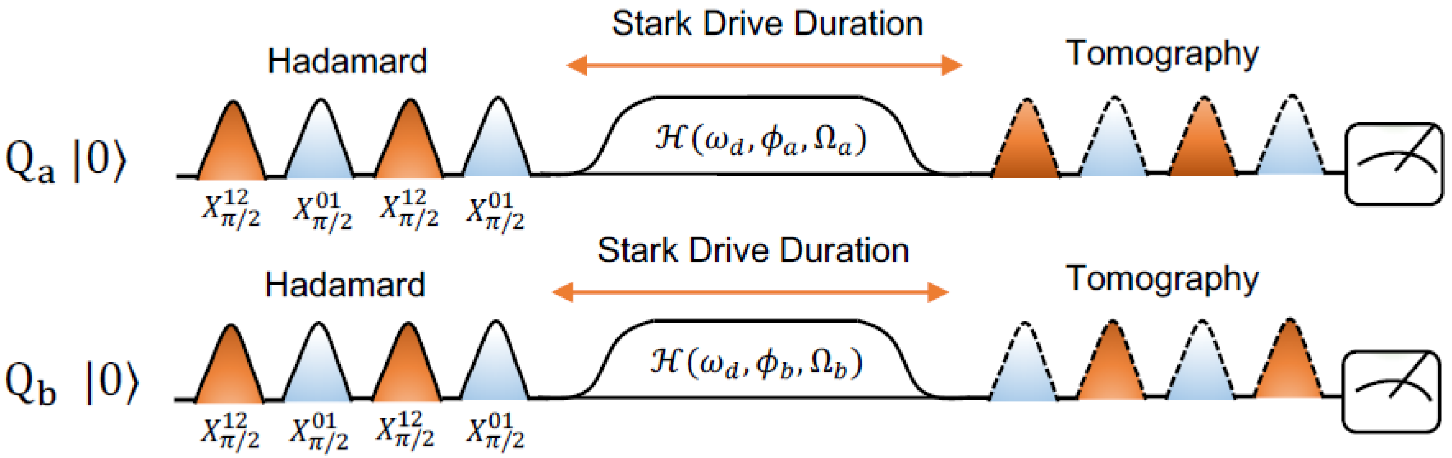

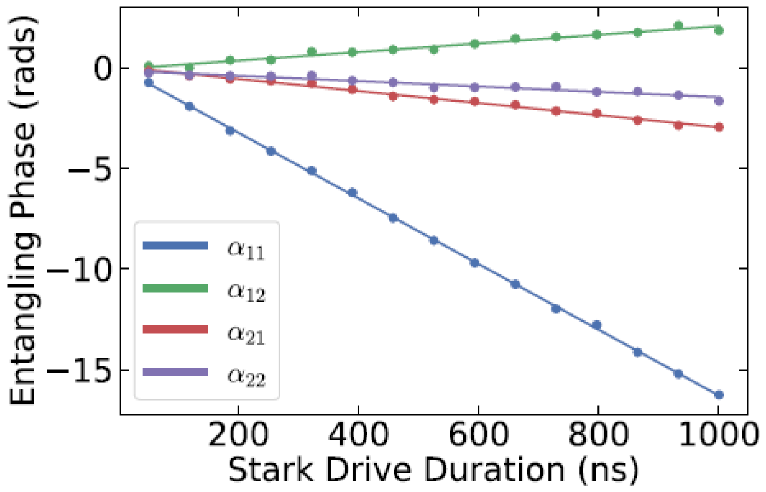

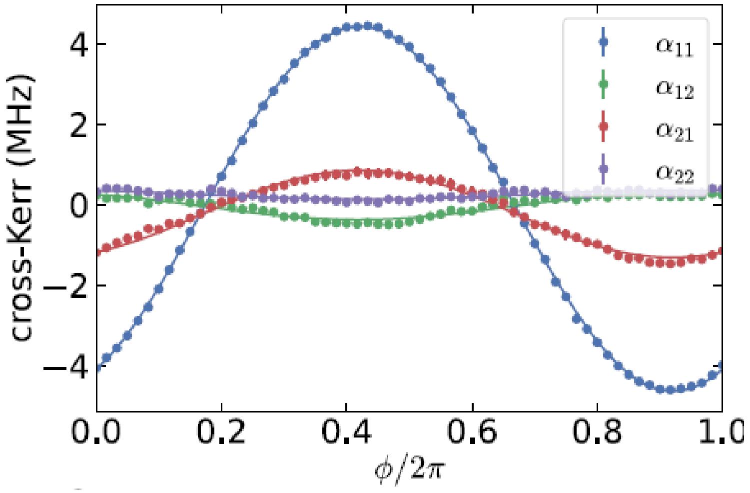

Characterizing the driven cross-Kerr

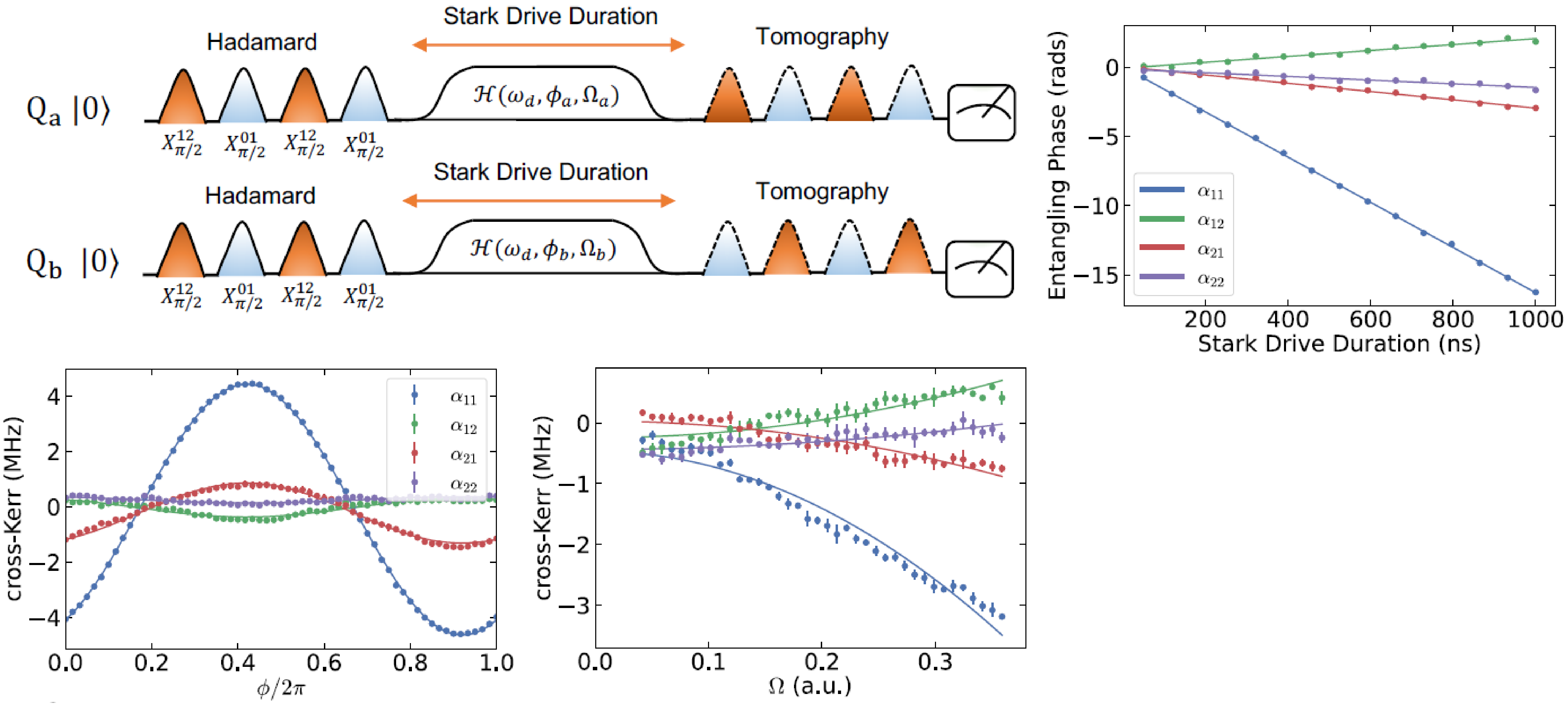

Characterizing the driven cross-Kerr

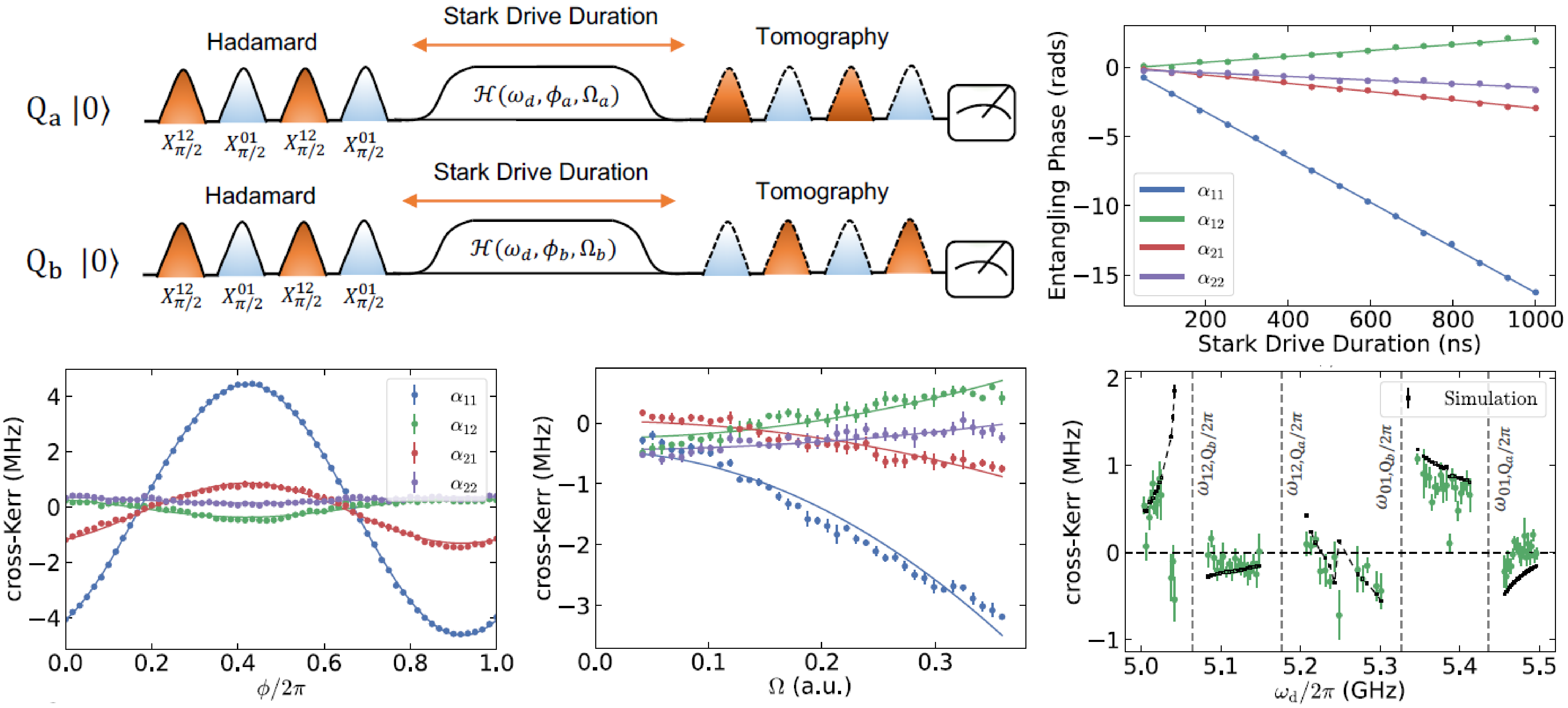

Characterizing the driven cross-Kerr

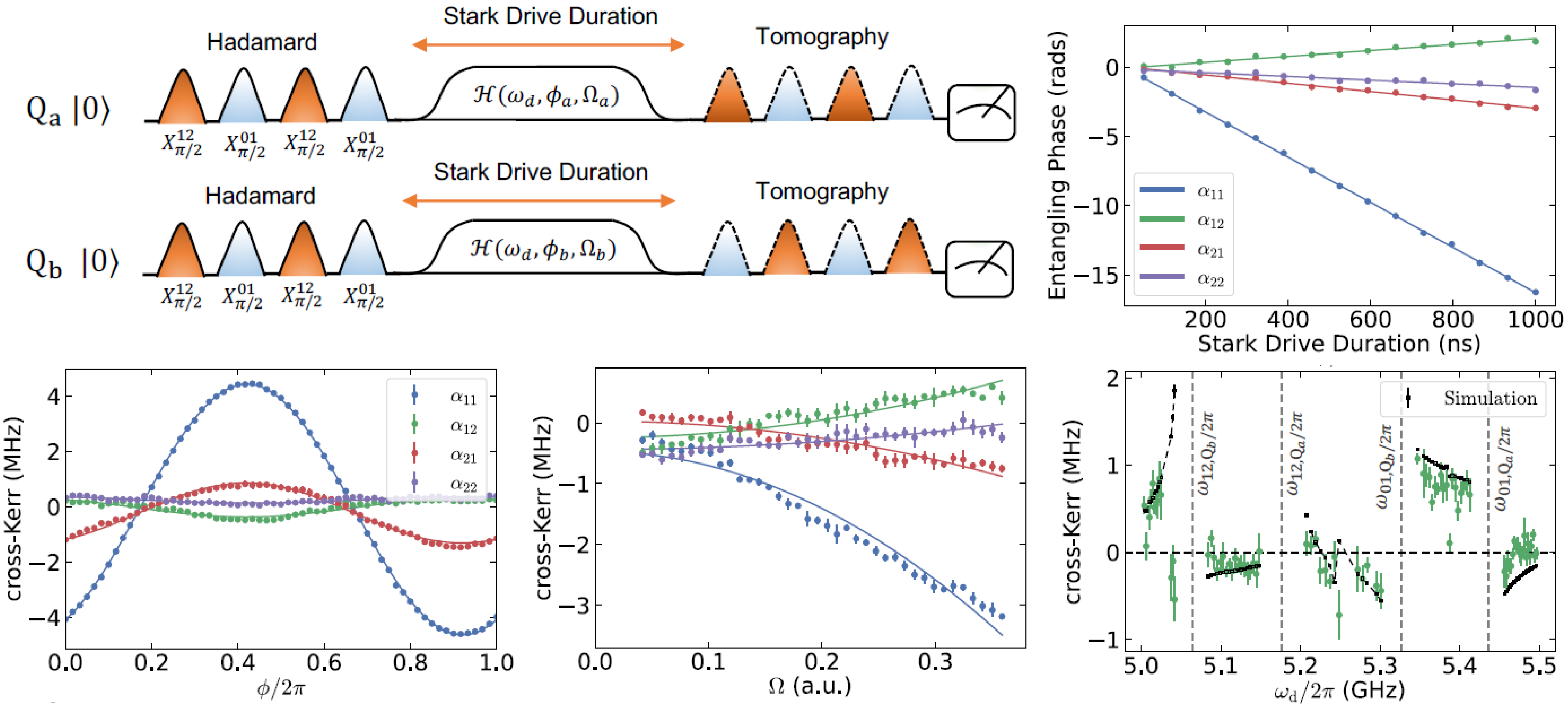

- Novel qutrit entangling interaction. Compared to static interaction, large increase in strength of cross Kerr interaction achievable, engineerable entangling phases.

Gate benchmarking

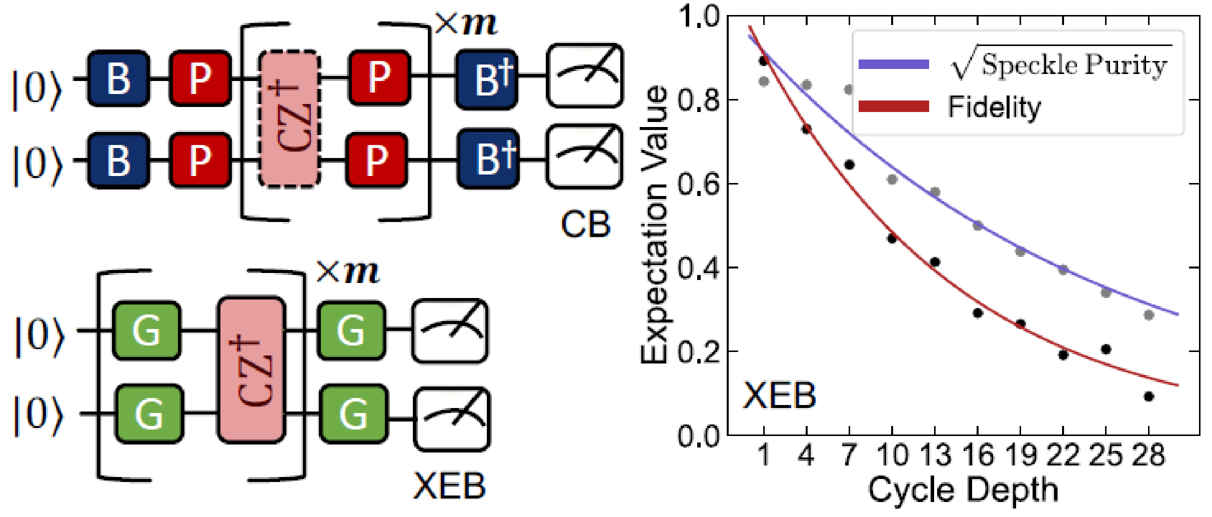

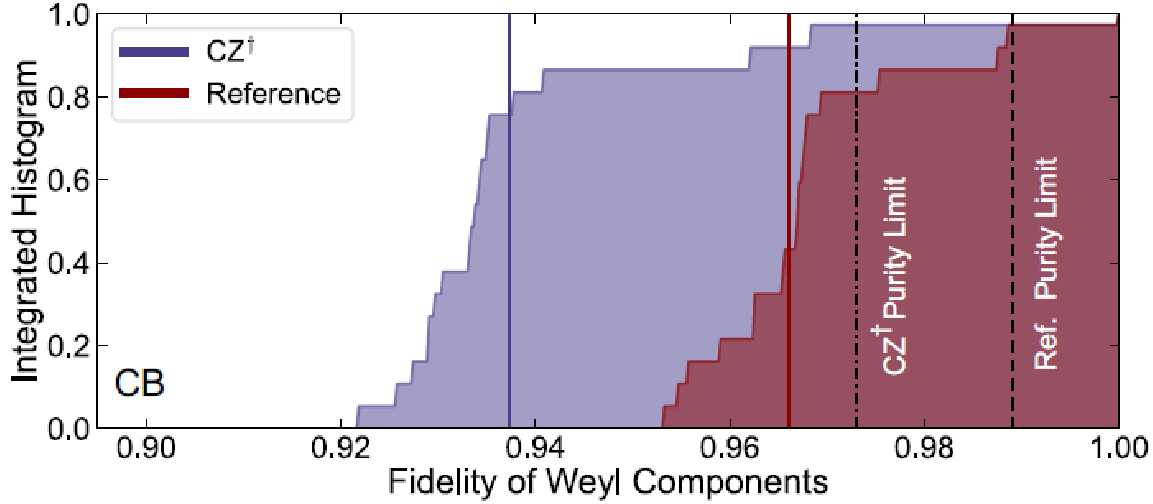

Pulse Sequence:

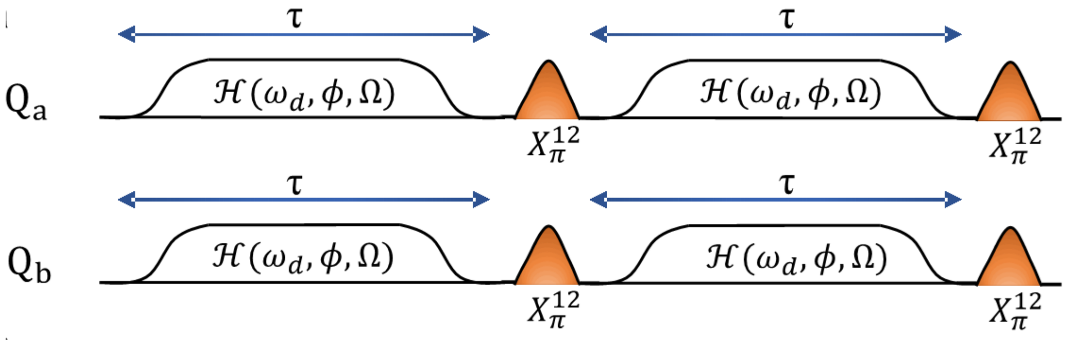

Gate benchmarking

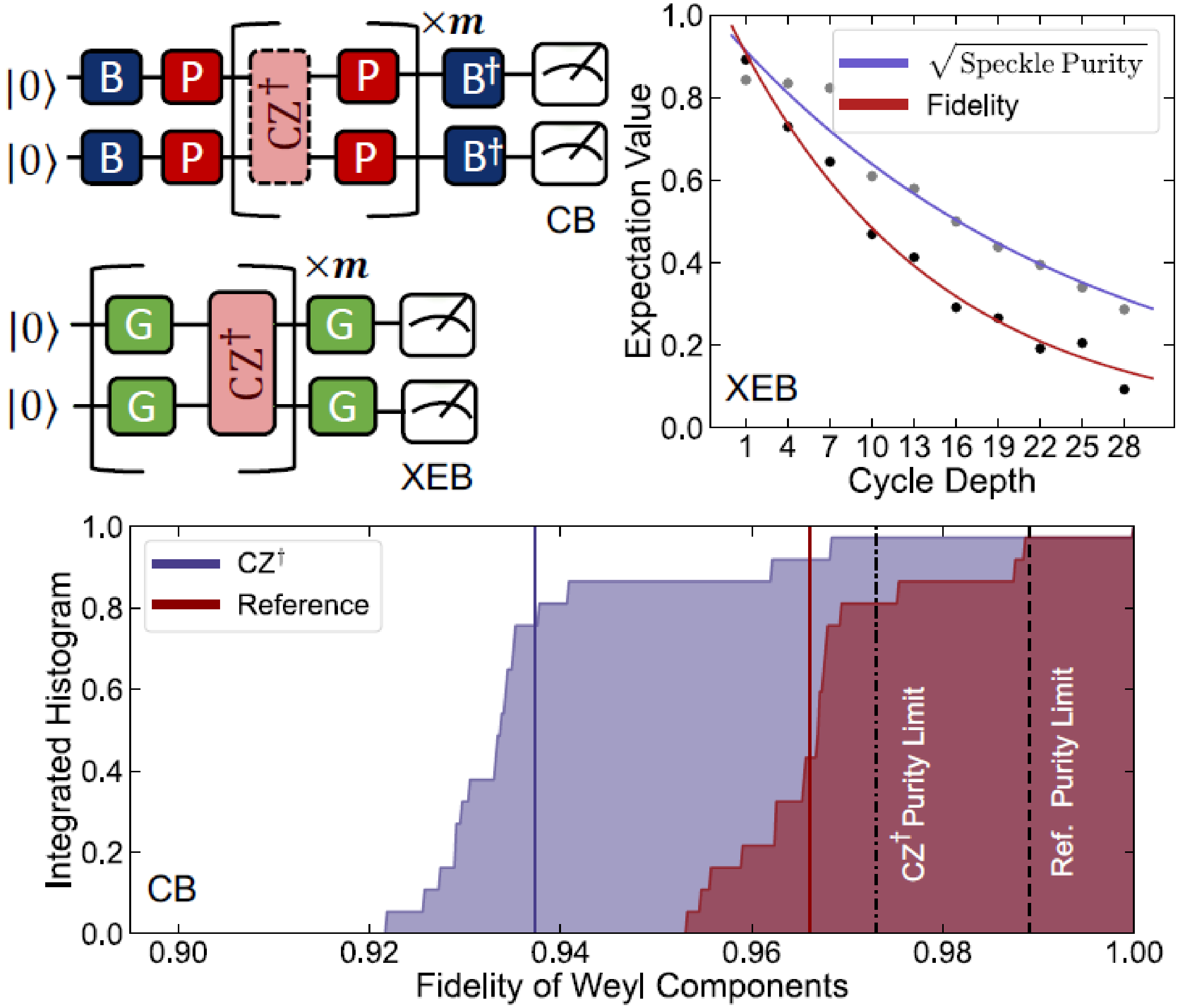

Pulse Sequence:

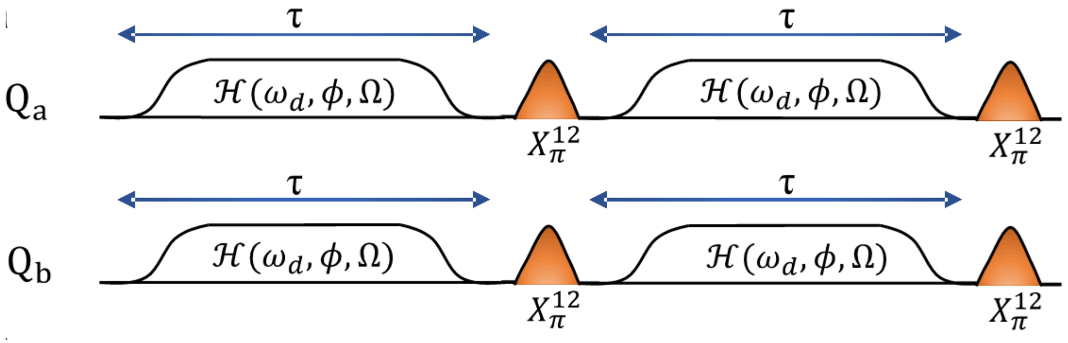

Cycle Benchmarking:

$$e_F = \frac{D-1}{D}\left(1 - \frac{\mathcal{F}_D}{\mathcal{F}_T}\right)$$

$$\mathcal{F}_T = 0.965 \pm 0.001$$
$$\mathcal{F}_D = 0.936 \pm 0.001$$

Gate benchmarking

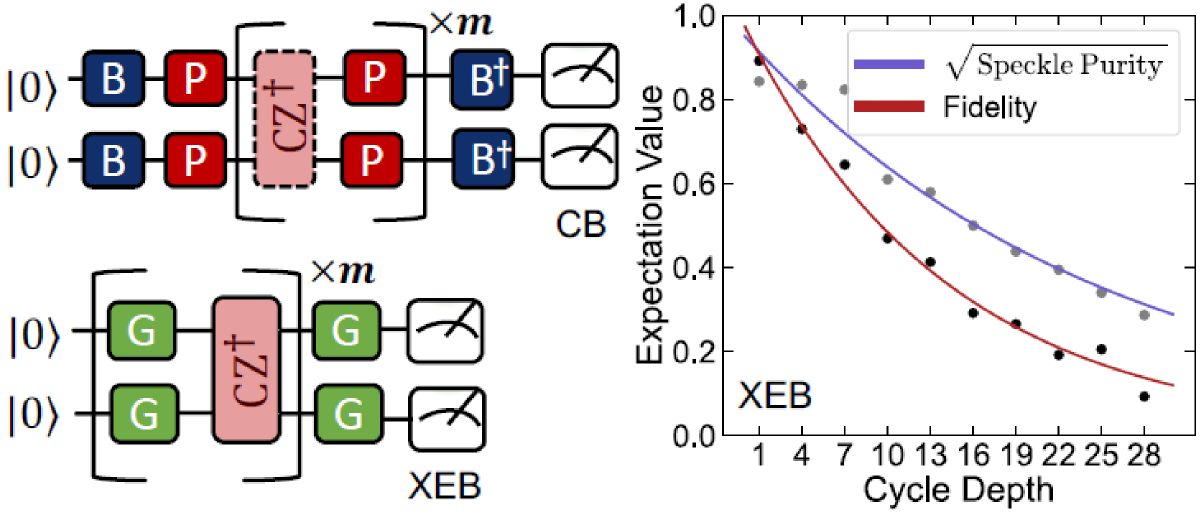

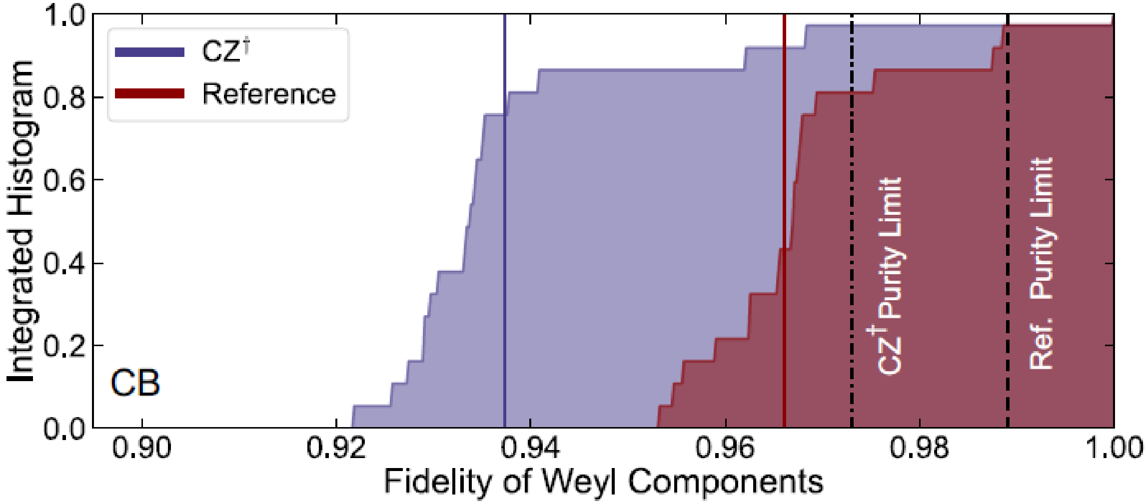

$$\mathcal{F}_{CZ^\dagger} = 0.973 \pm 0.001$$

Pulse Sequence:

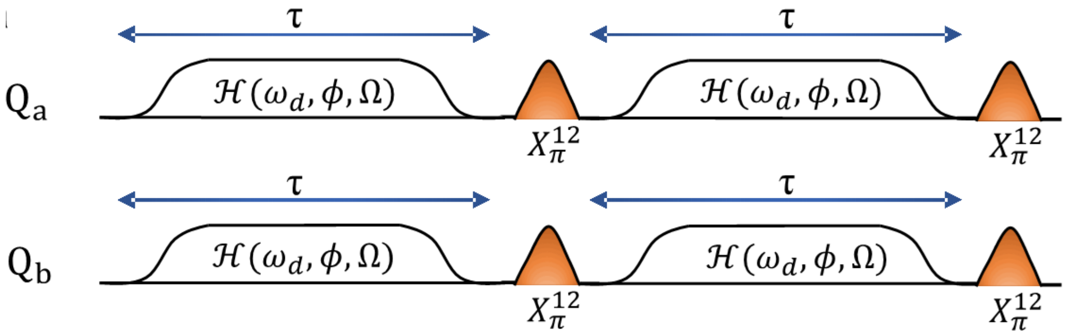

Cycle Benchmarking:

$$e_F = \frac{D-1}{D}\left(1 - \frac{\mathcal{F}_D}{\mathcal{F}_T}\right)$$

$$\mathcal{F}_T = 0.965 \pm 0.001$$
$$\mathcal{F}_D = 0.936 \pm 0.001$$

Gate benchmarking

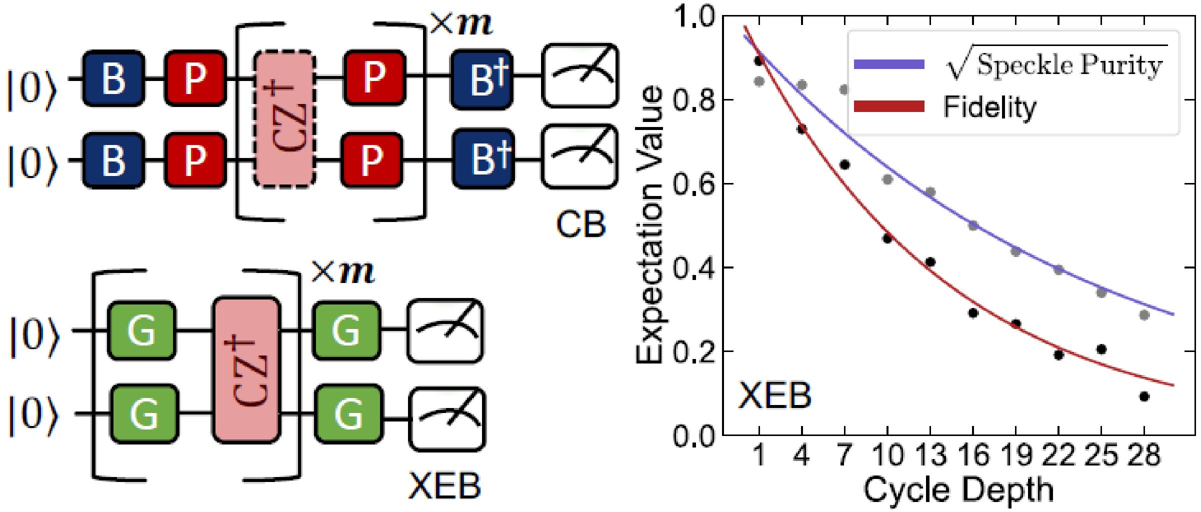

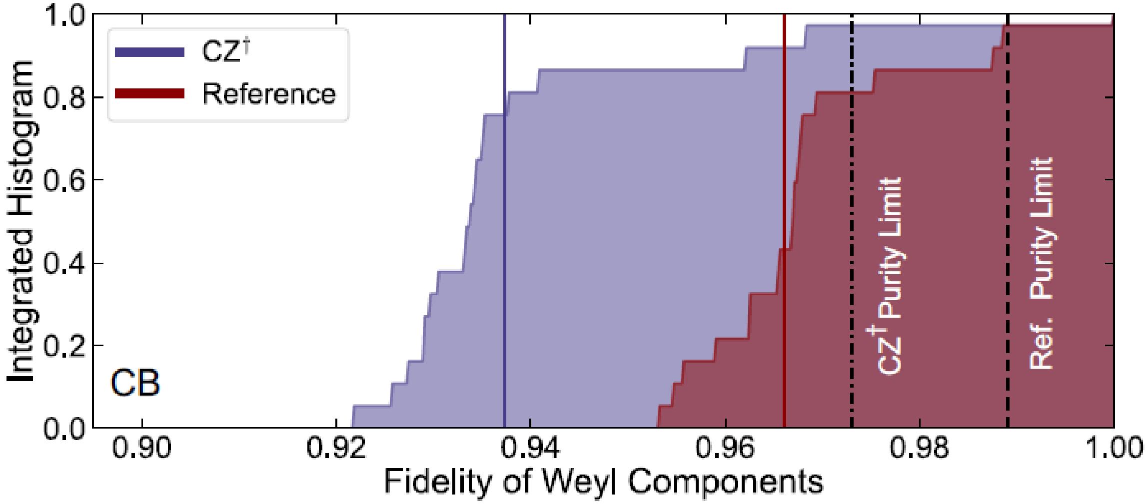

$$\mathcal{F}_{CZ^\dagger} = 0.973 \pm 0.001$$

Pulse Sequence:

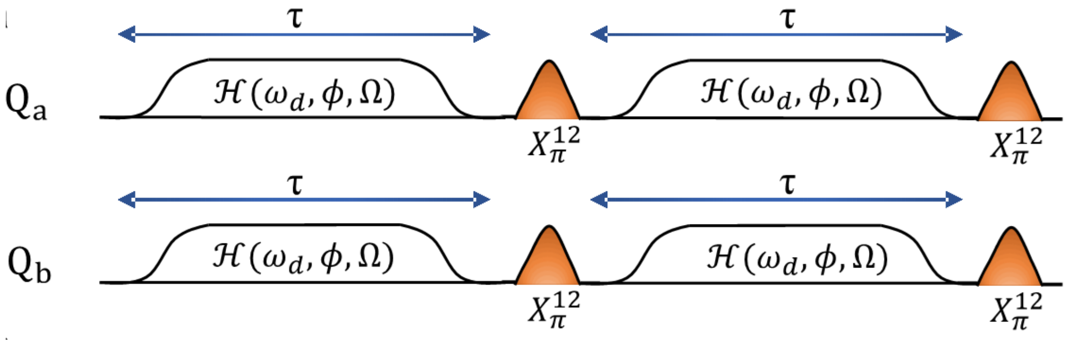

Cycle Benchmarking:

$$e_F = \frac{D-1}{D}\left(1 - \frac{\mathcal{F}_D}{\mathcal{F}_T}\right) \qquad \mathcal{F}_T = 0.965 \pm 0.001 \quad \mathcal{F}_D = 0.936 \pm 0.001$$

- Qutrit XEB agrees within a standard error of CB estimate of process infidelity of dressed cycle
  Arute *et al.* Nature. **574**, 505–510 (2019)
- New Benchmarking protocol developed
- Factor of 4 decrease in infidelity compared to past two-qutrit gates

Layered error mitigation with qutrits

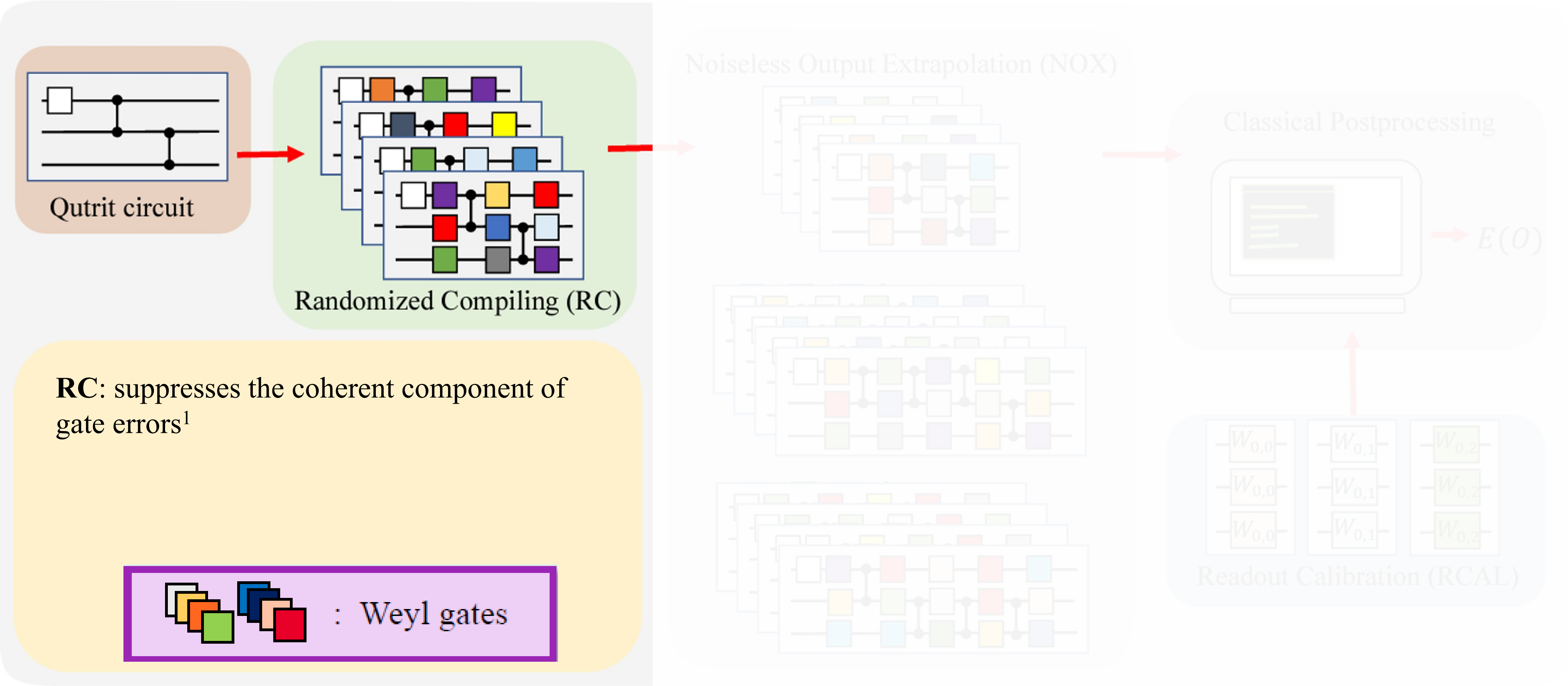

[1]Hashim PRX (2021), [2]Ferracin arXiv:2201.10672 (2022)

Layered error mitigation with qutrits

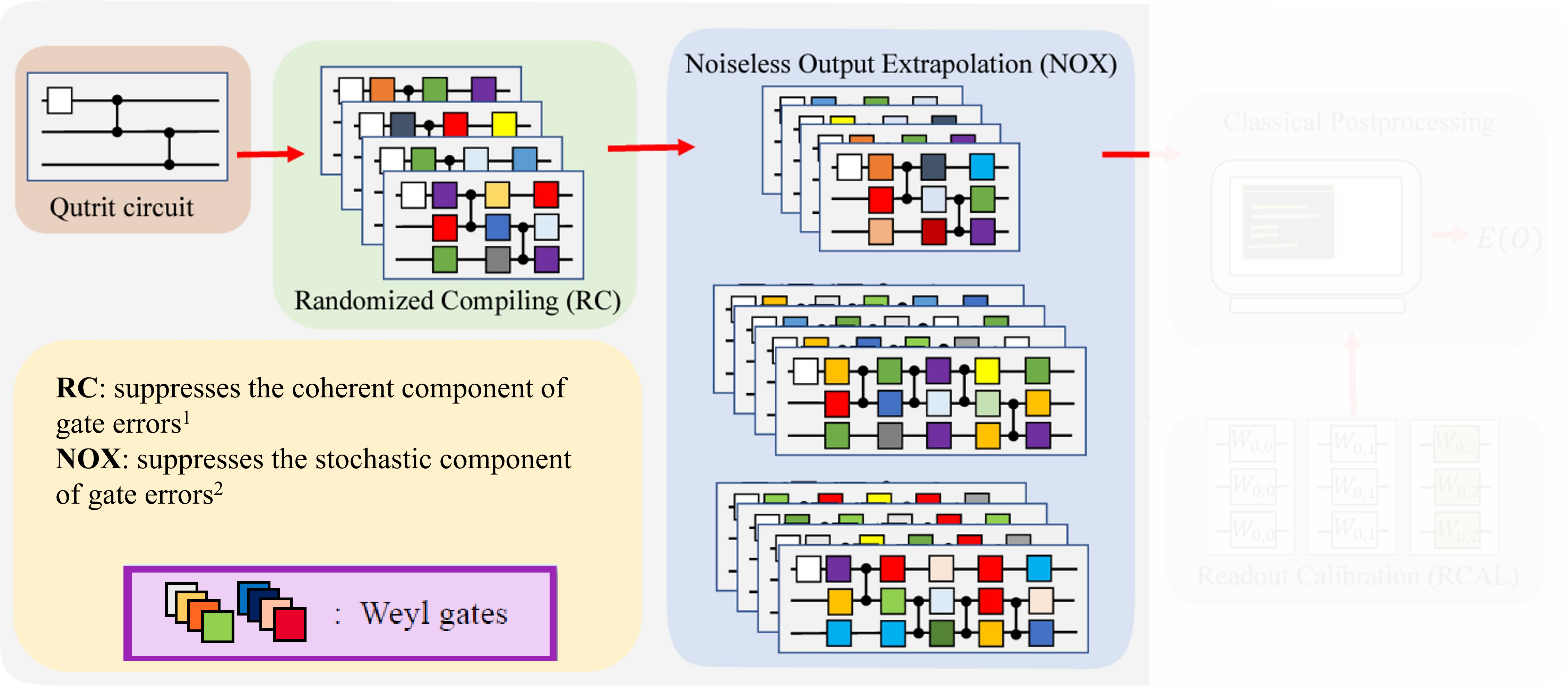

RC: suppresses the coherent component of gate errors[1]
NOX: suppresses the stochastic component of gate errors[2]

[1]Hashim PRX (2021), [2]Ferracin arXiv:2201.10672 (2022)

Layered error mitigation with qutrits

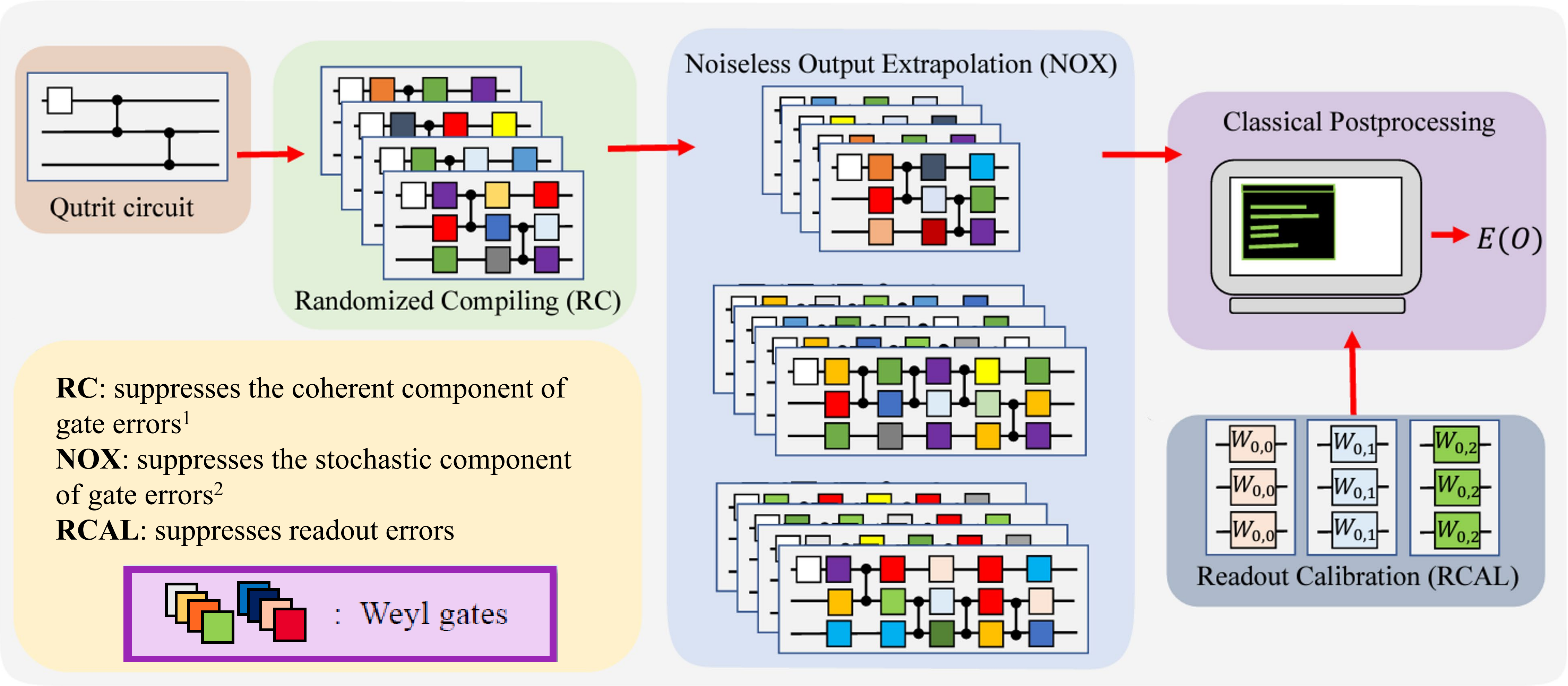

[1]Hashim PRX (2021), [2]Ferracin arXiv:2201.10672 (2022)

Highly entangled ternary quantum states

- To demonstrate multi-qutrit operations, we construct ternary GHZ states:

$$|\psi_{\mathrm{GHZ}}\rangle = \frac{|000\rangle + |111\rangle + |222\rangle}{\sqrt{3}}$$

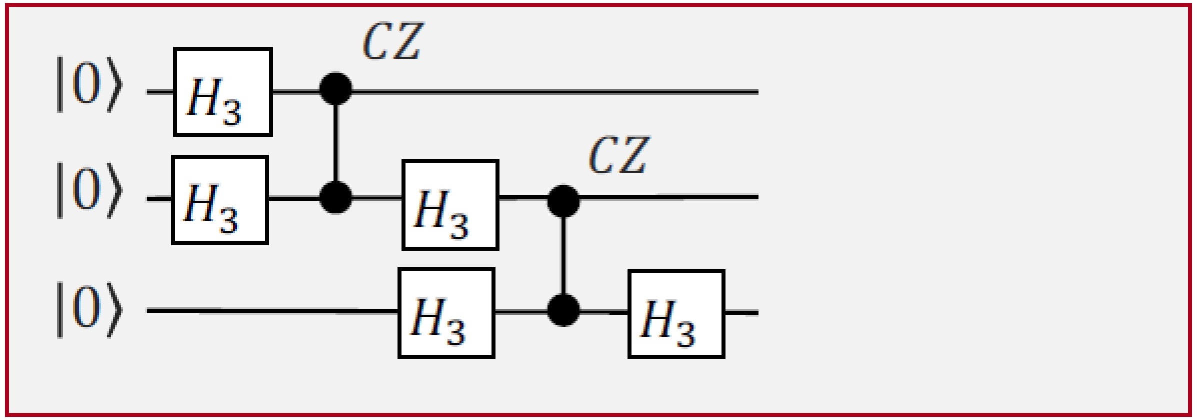

Highly entangled ternary quantum states

- To demonstrate multi-qutrit operations, we construct ternary GHZ states:

$$|\psi_{\mathrm{GHZ}}\rangle = \frac{|000\rangle + |111\rangle + |222\rangle}{\sqrt{3}}$$

- States characterized with tomography

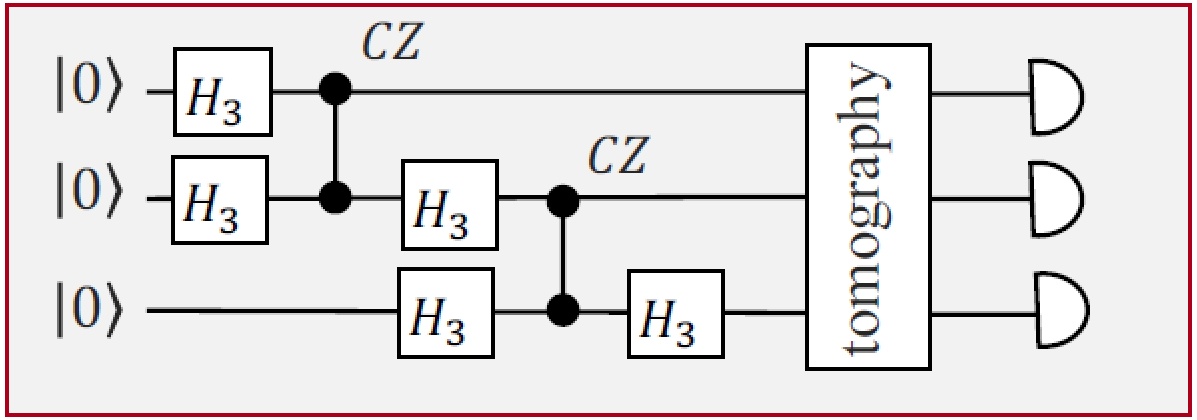

Highly entangled ternary quantum states

Noiseless simulation

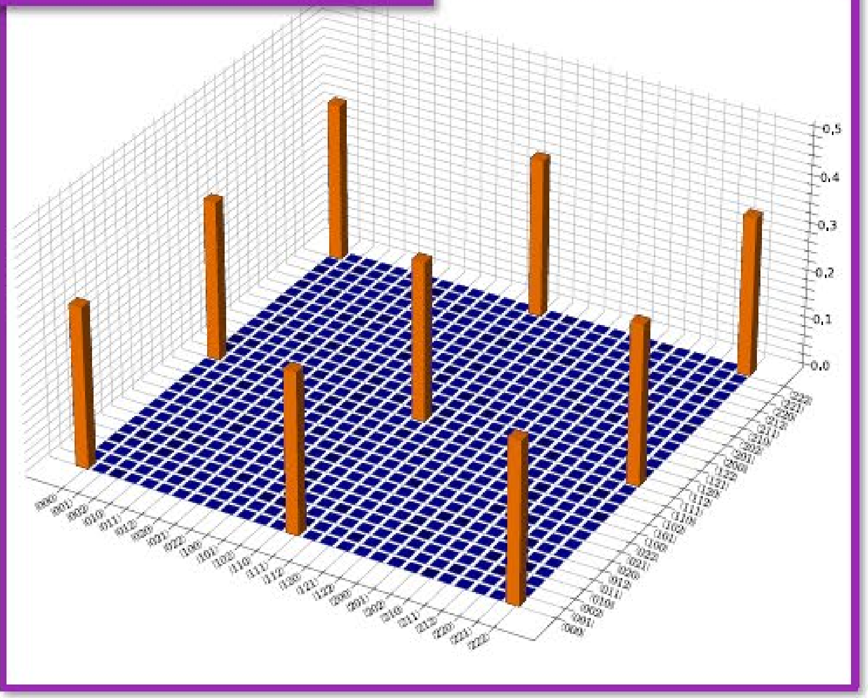

Unmitigated experiment

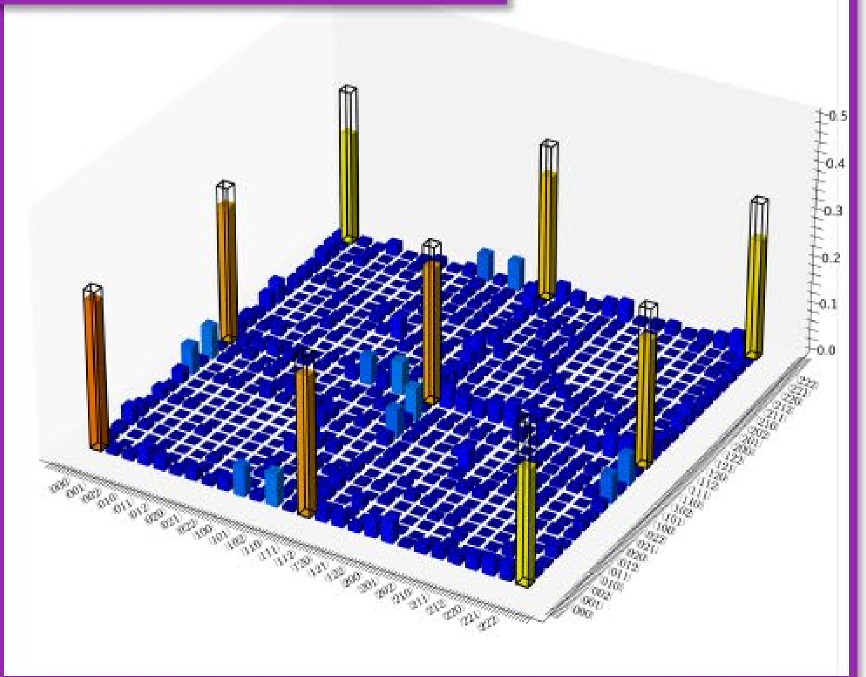

Infidelity of reconstructed state

def.: $\mathrm{IF}(\rho_{id}, \rho_{exp}) = 1 - \left(\mathrm{Tr}\sqrt{\sqrt{\rho_{id}}\rho_{exp}\sqrt{\rho_{id}}}\right)^2$

$\approx 18\%$

Highly entangled ternary quantum states

Noiseless simulation

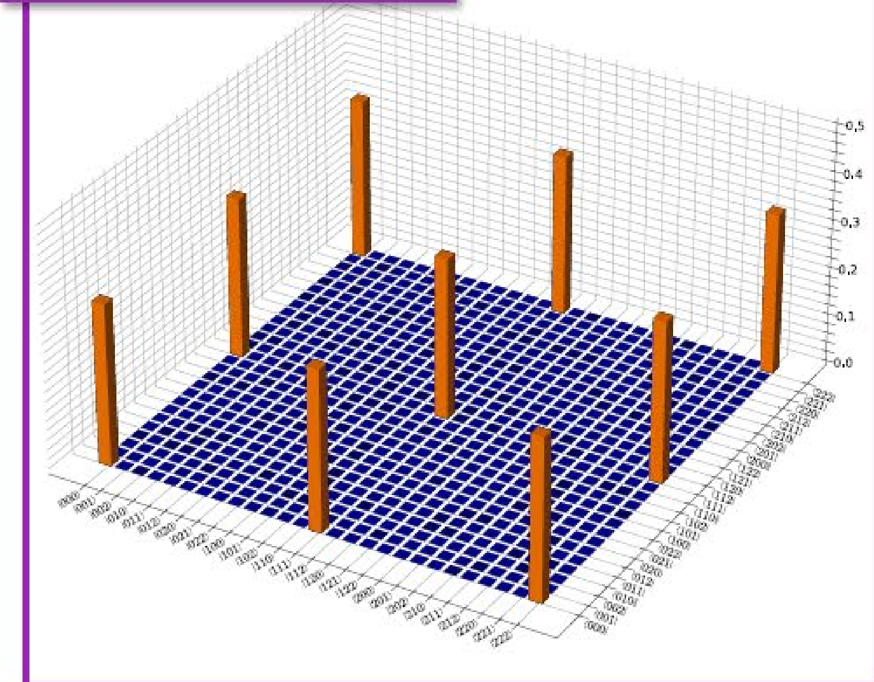

Mitigated experiment

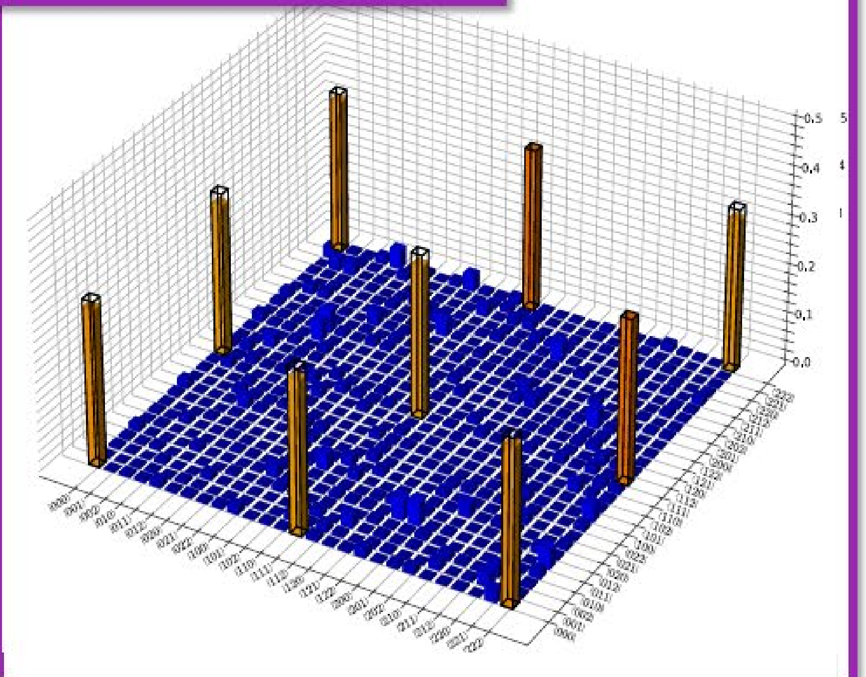

Infidelity of reconstructed state

def.: $IF(\rho_{id}, \rho_{exp}) = 1 - \left(\mathrm{Tr}\sqrt{\sqrt{\rho_{id}}\rho_{exp}\sqrt{\rho_{id}}}\right)^2$

$\approx 18\%$ → $\approx 5\%$

Improvements on random qutrit circuits

- Circuits alternating random single-qutrit gates and $CZ^\dagger$ gates

Improvements on random qutrit circuits

- Circuits alternating random single-qutrit gates and $CZ^\dagger$ gates
- To characterize the performance, we calculate the VD between ideal and experimental results

Variation Distance (VD)

def.: $\mathrm{VD}(p_{id}, p_{exp}) = \frac{1}{2}\sum_{\bar{s}} | p_{id}(\bar{s}) - p_{exp}(\bar{s}) |$

Improvements on random qutrit circuits

- Circuits alternating random single-qutrit gates and $CZ^\dagger$ gates
- To characterize the performance, we calculate the VD between ideal and experimental results

Variation Distance (VD)

def.: $\mathrm{VD}(p_{id}, p_{exp}) = \frac{1}{2}\sum_{\overline{s}} | p_{id}(\overline{s}) - p_{exp}(\overline{s}) |$

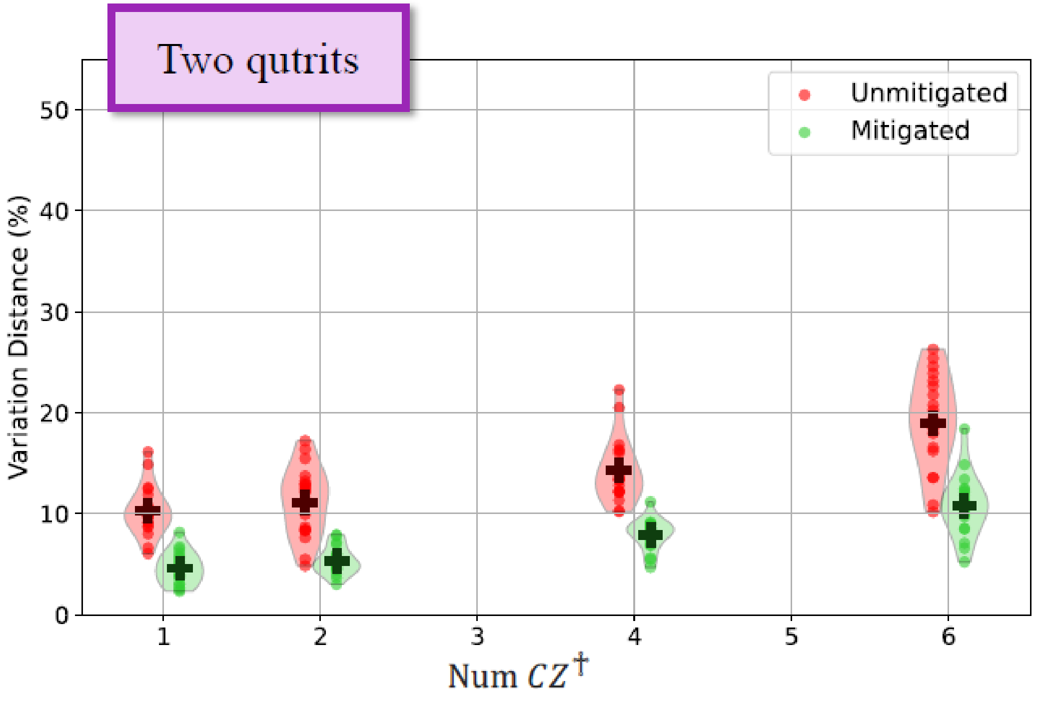

Improvements on random qutrit circuits

- Circuits alternating random single-qutrit gates and $CZ^\dagger$ gates
- To characterize the performance, we calculate the VD between ideal and experimental results

Variation Distance (VD)

def.: $\mathrm{VD}(p_{id}, p_{exp}) = \frac{1}{2}\sum_{\bar{s}} | p_{id}(\bar{s}) - p_{exp}(\bar{s}) |$

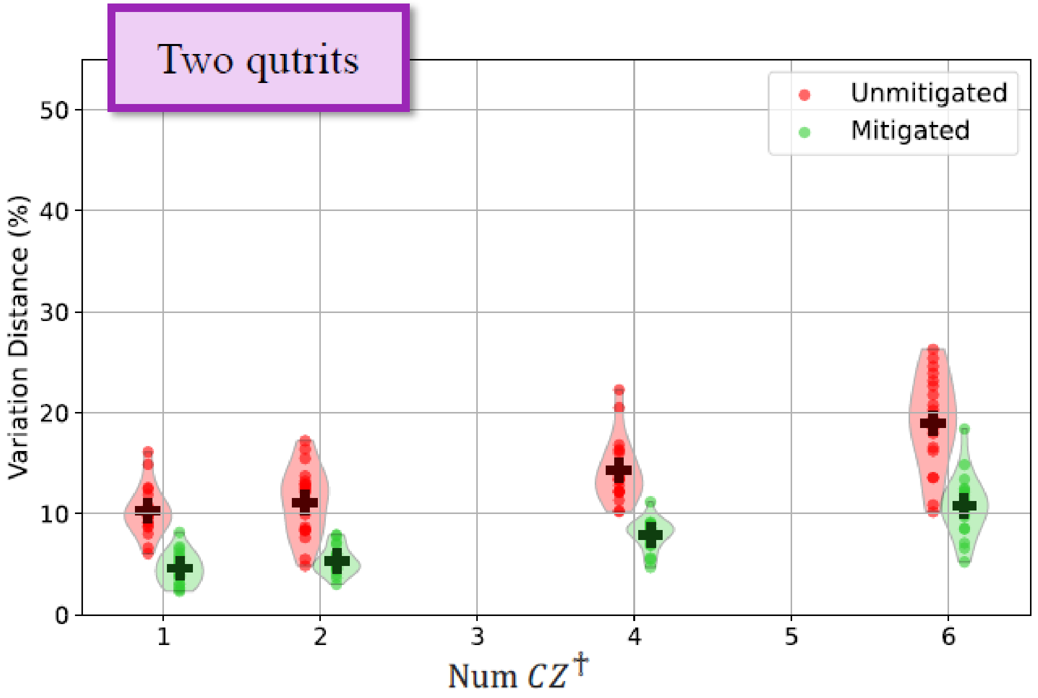

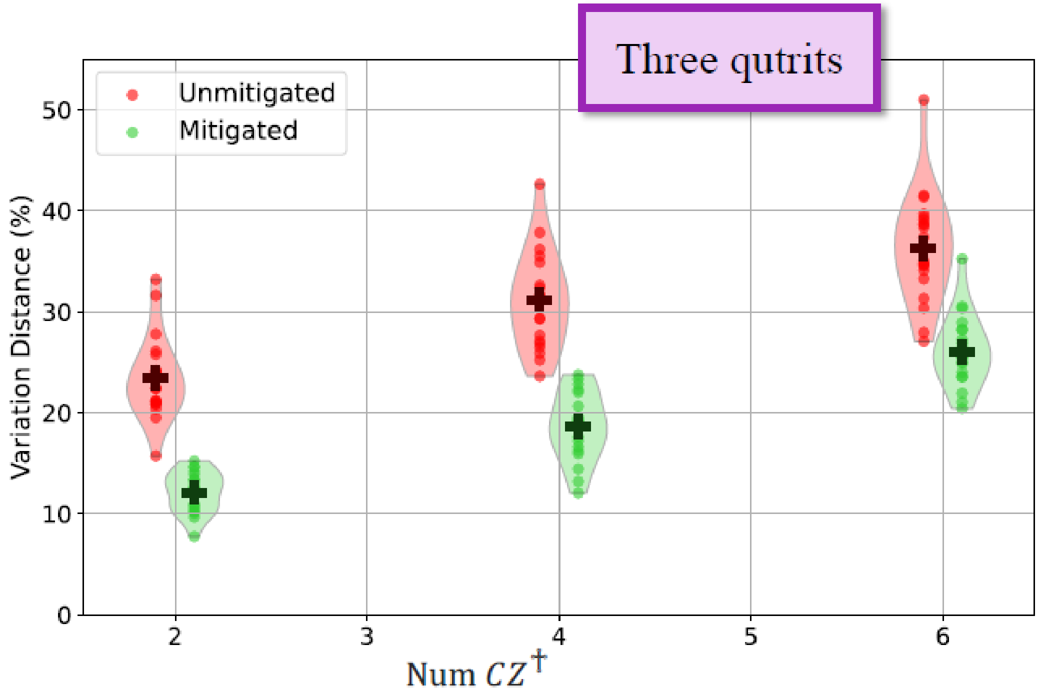

What's next with qutrits?

Noise tailoring and error mitigation

Basic demonstrations of ternary QEC

New approaches to multi-qubit gates

Cancellation of static cross-Kerr

(coupler/pulse)

Quantum simulation:

- Spin-1 interaction dynamics
- Quantum Chromodynamics
- Scaler QED[1]
- Neutrino flavor oscillations[2]
- Your ideas!

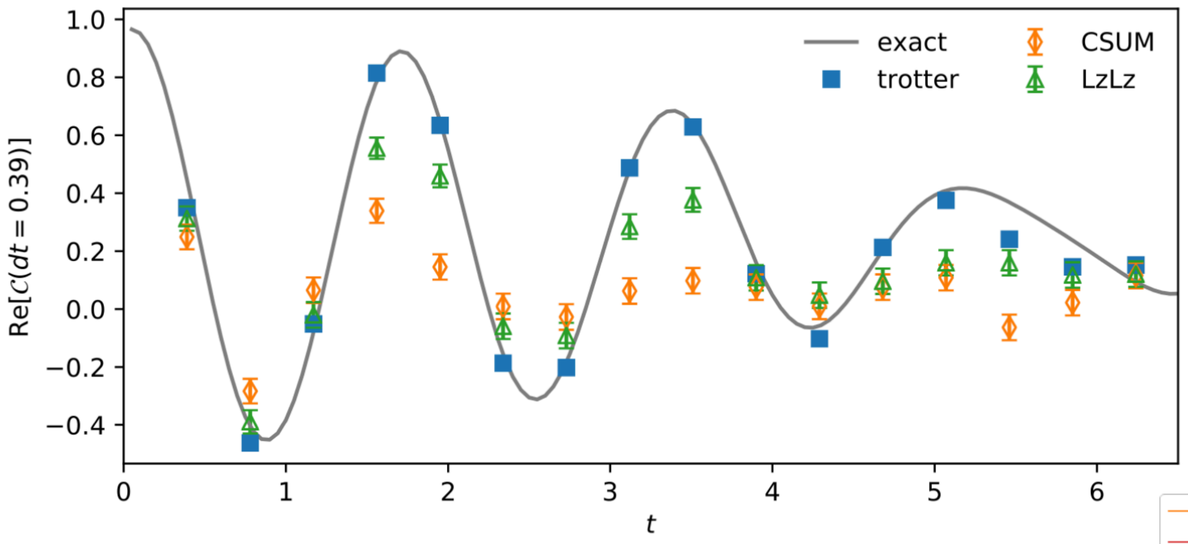

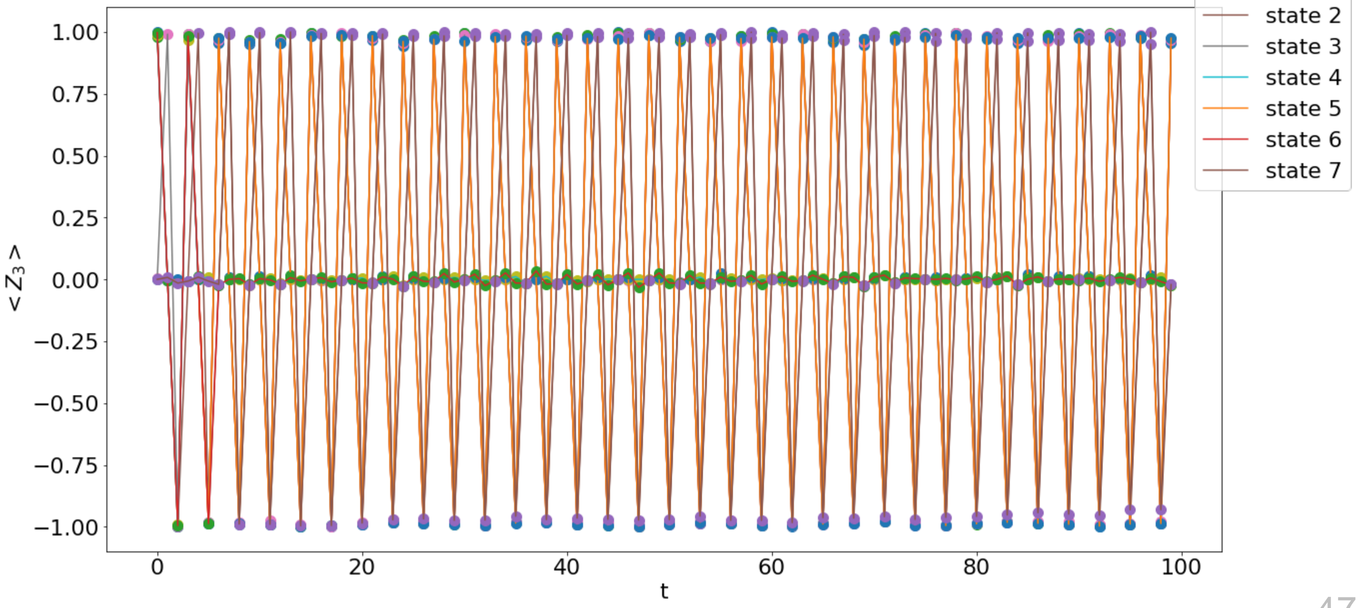

[1]Gustafson, arXiv:2201.04546 (2022)
[2]Nguyen, arXiv:2212.14170 (2023)

User Program

Enabling broad, impactful science with AQT resources

Open Quantum Resource

The AQT platform is open at no cost to teams from academia, industry, and government laboratories for projects with significant scientific value and high potential impact to QIS.

Flexibility for Users

The system was designed to allow easy access and modification at any point in the quantum computation stack, from the quantum processor design to the high-level software interface.

Exchange of Best Practices

AQT's platforms incorporates advances developed from internal research and user projects, making them broadly available to the QIS research community.

Developing QIS Workforce

Broadens the availability of cutting-edge quantum hardware to new generations of scientists and engineers at a a broad range of institutions.

User Projects – Proposal and Review

AQT runs an annual widely-announced Open Call – typically announced in the Fall

The proposal process is designed to have low barriers to entry with brief LOIs and proposals. Technical staff members are available throughout the proposal process to answer questions and discuss the feasibility of potential project ideas.

Review criteria:

- Scientific merit
- Alignment with AQT program goals and use of unique resources not available in the commercial domain
- Feasibility with testbed capabilities and resources

Project areas:

- Implementations of quantum algorithms or quantum simulations
- Quantum characterization, validation, and control routines
- Novel control hardware / firmware / software
- Novel superconducting quantum processor architectures

User Projects – Lifecycle

Deep collaborations to maximize the scientific impacts of projects

Scoping → **Queue** → **Execution** → **Publication**

Scoping
Initial meetings of project and AQT teams to identify requirements

Queue
Execution order is based on resource and staff availability

Execution
Experiments are run by AQT staff in close collaboration with users

Publication
Results are typically jointly published by AQT and users

- Accepted proposals typically run over a period of 3-12 months, with frequent meetings between AQT staff and user teams.
- Experiments often evolve to incorporate new techniques or promising scientific directions.
- AQT projects are typically intended for publications in the academic literature, and resources are provided at no cost to users.

Berkeley team and collaborators

AQT

Akel Hashim
Ravi K. Naik
Alexis Morvan
Jean-Loup Ville
Bradley Mitchell
Trevor Chistolini
Christian Jünger
Larry Chen
Linus Kim

Noah Goss
John Mark Kreikebaum
Marie Lu
Kasra Nowrouzi
Ahmed Hajr
Long Nguyen
Zahra Pedramrazi
Noah Stevenson
Brian Marinelli

Kan-Heng Lee
Bingcheng Qing
Ke Wang
Karthik Siva
Gang Huang
Yilun Xu
Neelay Fruitwala
Wim Lavrijsen
Anastasiia Butko

Abhi Rajagopala
Ed Younis
Marc Davis
Ethan Smith
Costin Iancu
Chris Spitzer
Jonathan Carter
David I Santiago
Irfan Siddiqi

KEYSIGHT

Ian Hincks
Joel J. Wallman
Joseph Emerson

quantum benchmark

Samuele Ferracin
Arnaud Carignan-Dugas
Hammam Qassim

Infleqtion

Rich Rines
Victory Omole

SUPER.TECH

Frederic T Chong
Pranav Gokhale

Relevant Articles:

“High-fidelity qutrit entangling gates for superconducting circuits”, N. Goss, et. al., Nature Communications 13 (1), 7481 (2022)

“Extending the Computational Reach of a Superconducting Qutrit Processor”, N. Goss, et. al., arXiv:2305.16507 (2023)